AFFDL-TR-68-123

ANALYSIS OF THE ELASTIC CONTACT OF A HOLLOW BALL WITH A FLAT PLATE

JOHN H. RUMBARGER

R. CLYDE HERRICK

Franklin Institute Research Laboratories

FOREWORD

This final technical report was prepared by the Franklin Institute Research Laboratories, Philadelphia, Pennsylvania, under USAF Contract No. F33(615)-68-C-1205. The contract was initiated under Project No. 1315, "Bearings and Special Components", Task No. 131502, "Rational Bearing Design and Special Components". The contract was administered by the Air Force Flight Dynamics Laboratory, Air Force Systems Command, Wright-Patterson Air Force Base, Ohio, Mr. Phillip R. Eklund (FDFM), Project Engineer.

Mr. John H. Rumbarger, Senior Staff Engineer and Chief of the Large Structures and Rolling Element Bearing Section, Friction and Lubrication Laboratory, Mechanical and Nuclear Engineering Department of the Franklin Institute Research Laboratories was responsible for the execution of the problem. Mr. R. C. Herrick, Senior Research Engineer, Applied Mechanics Laboratory, Mechanical and Nuclear Engineering Department, was responsible for formulation of the finite-element computer solution. Messrs. F. Bogden, R. Keighley and Mrs. L. Holmes, Applied Mechanics Laboratory, were responsible for computer execution and data reduction.

This report covers work performed during the period 1 January 1968 through 31 May 1968. It was submitted by the authors in July 1968.

Information in this report is embargoed under the Department of State International Traffic in Arms Regulations. This report may be released to foreign governments by departments or agencies of the U. S. Government subject to approval of the Air Force Flight Dynamics Laboratory, or higher authority within the Department of the Air Force. Private individuals or firms require a Department of State export license.

Publication of this report does not constitute Air Force approval of the report's findings or conclusions. It is published only for the exchange and stimulation of ideas.

This report has been reviewed and is approved.

KENNERLY H. DIGGES
Chief, Mechanical Branch
Vehicle Equipment Division
AF Flight Dynamics Laboratory

ABSTRACT

The objective of this program was to conduct a preliminary analytical investigation of the stress field in a hollow sphere in the vicinity of the contact area. The sphere is subjected to a normal load applied through a flat plate. The elastic contact shape and extent were developed for a load of 1000 lb. applied to a one-inch diameter hollow ball with a 0.08 inch thick wall. Comparison of the maximum value and location of the reversing orthogonal subsurface shear stress with classical solid ball data according to the Lundberg-Palmgren dynamic life theory results in a 91.6% life reduction estimate for the hollow ball contact.

TABLE OF CONTENTS

LIST OF FIGURES

LIST OF FIGURES (CONT'D)

LIST OF TABLES

SECTION I

INTRODUCTION

The United States Air Force Flight Dynamics Laboratory is conducting test programs to determine the load-deflection characteristics (Ref. 1), fabrication development (Ref. 2), as well as other properties of a hollow ball for use in rolling element bearings. A hollow ball of proper design and manufacture possesses important potential advantages over a solid ball for certain specific bearing applications.

Large diameter radar-scanning antenna azimuth bearings and supersonic aircraft wing pivot bearings are cited (Ref. 1 & 2) as bearing applications which would derive a major advantage from the reduced weight of large diameter hollow balls.

High speed gas turbine engine and aircraft transmission bearings where the centrifugal and gyroscopic forces of solid-balls result in "skidding damage" and drastically reduced bearing life are also excellent applications for hollow balls (Ref. 3). The fast shaft speeds of modern gas turbine engine mainshafts require a high-speed thrust ball bearing and the use of hollow balls to overcome inertial effects and reduce weight appear attractive to many engine designers. Such ball thrust bearings would tend to achieve improved internal ball load distribution and hence greater fatigue life than bearings having solid balls.

This report represents the first analytical work undertaken to describe the complicated subsurface stress field which results from the interaction of the stresses resulting from the small but finite Hertz type contact and the hollow sphere bending stresses. Obviously a hollow ball must have a sufficiently long fatigue life in the contact area before the advantages of reduced inertia and gyroscopic effects may be realized.

The use of hollow balls in rolling element bearings cannot be relegated to the realm of the bizarre. Aircraft engine ball thrust bearing requirements are continually expanding and anticipated 3.0×10^6DN operating conditions cannot be met by present solid or conventional ball designs. (DN is a speed factor which is used to express high speed bearing operational requirements and consists of the bore of the bearing, D, expressed in millimeters times the rotating shaft speed, N, expressed in revolutions per minute.)

SECTION 2

SUMMARY

The elastic contact of a one-inch diameter hollow ball in contact with a flat plate under one thousand pounds normal load is analyzed by means of a finite-element digital computer program. The shape of the contact surface is gradually developed under increasing increments of normal load which brings successively greater areas of the mathematical model into contact. The shape of the final contact zone and the surface contact stress distribution are obtained. Superposition of the incremented finite-element solutions enables a determination of the complex three dimensional subsurface stress field which results from the interaction of the classical HERTZ type contact problem and the hollow sphere internal bending stresses.

A wall thickness of 0.08 inch was used throughout the analysis. (Diameter to thickness ratio of 12.5). The radius of the computed circular contact area correlated within 1-1/2% of experimental hollow ball compression tests. The hollow ball solution was then compared with classical solid ball contact solutions in order to estimate the relative effects of the hollow ball internal stress field.

The hollow ball contact with a flat plate results in a larger radius of contact but with no significant change in the maximum Hertz compressive contact stress. The maximum unidirectional subsurface shear stress located along the line of centers (axis of symmetry) is significantly less in the hollow ball. The maximum reversing orthogonal subsurface shear stress, which is assumed to be the decisive stress amplitude for life calculations is found to be greater in magnitude and located nearer to the contact surface in the hollow ball contact.

A 91.4 percent reduction in the contact fatigue life is predicted for the specific hollow ball which was analysed. This life reduction would rapidly reduce as the wall thickness of the ball is increased.

The method of finite-element computer solution of the elastic contact problem was successful and reasonable three dimensional subsurface stress fields were described. Additional analysis is required to optimize hollow ball life as a function of wall thickness and weight reduction. The interaction of the contact stresses and the shell bending stresses have a significant effect upon predicted performance.

SECTION 3

METHOD OF COMPUTER SOLUTION

An existing and operating FIRL digital computer program using the "finite element" method of solution for determining stresses and displacements developed in composite axisymmetric solids of arbitrary geometry subjected to axisymmetric thermal or mechanical loads was used for the solution of the contact of a hollow ball on a flat plate (Ref. 4). The "finite element" method is a general method of structural analysis in which a continuous structure is replaced by a finite number of elements interconnected at a finite number of nodal points. This type of idealization is inherent in the conventional analysis of frames and trusses. An assembly of different sizes of triangular and rectangular rings interconnected at a finite number of nodal points (joints) is used to represent the continuous structure as shown in Fig. 1. Loads acting on the system are replaced by statically equivalent concentrated forces acting at the nodal points of the finite element system. Continuity between elements of the system is maintained by requiring that within each ring element "lines initially straight remain straight in their displaced position." The governing differential equations for linear elastic theory have been known for many years, yet closed form solutions have been obtained for only a limited number of systems. The use of matrix techniques allow the rapid simultaneous solution of finite element systems with as many as 1000 nodal points. The resulting solution yields stresses and displacements throughout the hollow ball and flat plate so that a true three dimensional stress field is obtained.

The main difficulty which had to be overcome was the fact that we did not know the profile of the contact surface or the distribution of the Hertz compressive stresses over the contact. All that was known was that the limit of the contact area would be a circle because of the axisymmetric type of structure and loading. Two approaches were considered to obtain to the contact problem.

1. A grid of triangular and rectangular rings such as shown by nodal points may be described as depicted in Fig. 1 with the ball touching the flat plate at one or two nodal points. Small increments of load are applied to the system and the nature of the displacement of the common nodal points between ball and plate are observed after each computer solution. As the load is gradually increased (one computer run is required for each load step) the resulting displacements are examined. Increased in load will gradually bring additional surface nodal points into contact because of the increased zone of contact. The boundary condition input to the problem is changed after each run and gradually a contact zone is developed step by step which will be a truly compatible solution to the

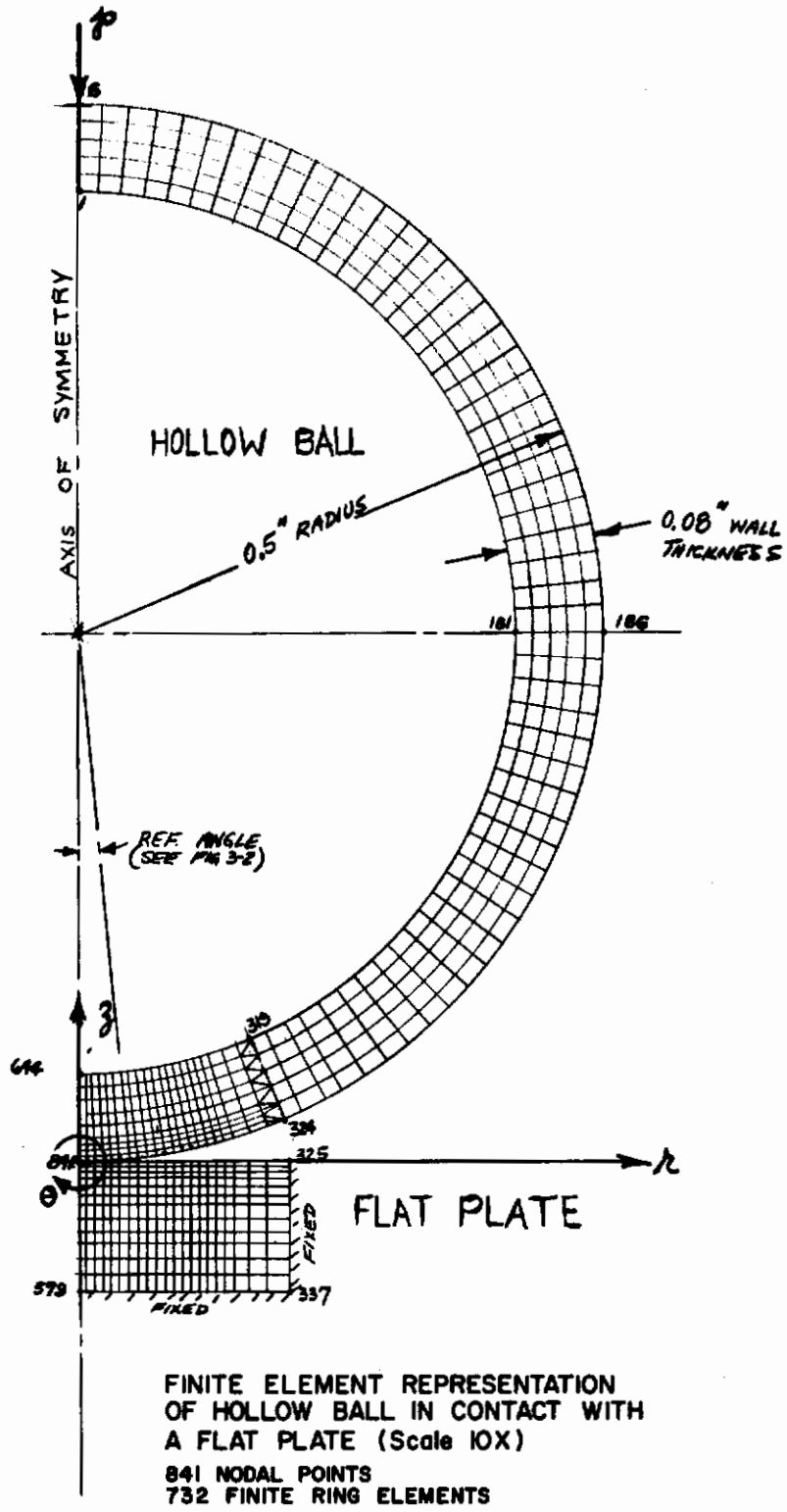

FINITE ELEMENT REPRESENTATION OF HOLLOW BALL IN CONTACT WITH A FLAT PLATE (Scale 10X)

841 NODAL POINTS
732 FINITE RING ELEMENTS

Fig. 1 - Model 1 Coarse Grid.

equations of elasticity for the ball and the plate in common contact. The shape, extent and profile of the contacting surface will be known and the stress distribution will be described. The stresses and displacements at each nodal point in the system will also be known.

2. The second method of matching solutions between the ball and the plate to obtain the required shape, extent and profile of the contact would treat the ball and plate separately. A grid as shown in Fig. 1 would be used. A known load pattern such as the hemispherical stress distribution of the classical solution of a solid ball on a flat plate would be applied independently to both the ball and the plate. This known loading would be solved by the finite element method and the contact surface displacements would be described for each body. They would not match and a correction would be required. Influence coefficients would be developed by applying ring loads successively to each nodal point of each body along the anticipated contact surface. These influence coefficients would be used in matrix form to calculate an applied load distribution which would be required to reduce the errors in the displacement patterns of the ball and the plate to zero. This type of iterative approach used for approximately three or four times would result in a matching solution in the contact zone.

The first method, described above was used to obtain the solutions presented in this report. Fig. 1 illustrates the first coarse-grid mathematical model (Model 1) which was used to represent the contact of a hollow ball on a flat plate. A total of 732 finite ring elements consisting of 841 nodal points were needed. The spacing radially along the contact surface was in 0.008 inch increments. Thus the 1000 pound load produced a contact radius somewhere between 0.024 inch and 0.032 inch. Only three nodal points at the ball-plate surface came into common contact at radii of 0.008, 0.0016, and 0.024 inches. This solution was useful in describing the subsurface stress pattern along the axis of symmetry but was not capable of accurately refining the radius of contact or the subsurface stress field throughout the three-dimensional subsurface vicinity of the contact. Results of the analysis of Model 1 are discussed in Section 4.

A new mathematical model was devised with closer grid spacing in the radial direction in order to obtain more accurate contact stress and subsurface stress information. Fig. 2 shows the portion of Model 2 with the closer spacing. The radial spacing was reduced to 0.004 inch up to a radius of 0.032 inch from the axis of symmetry. The

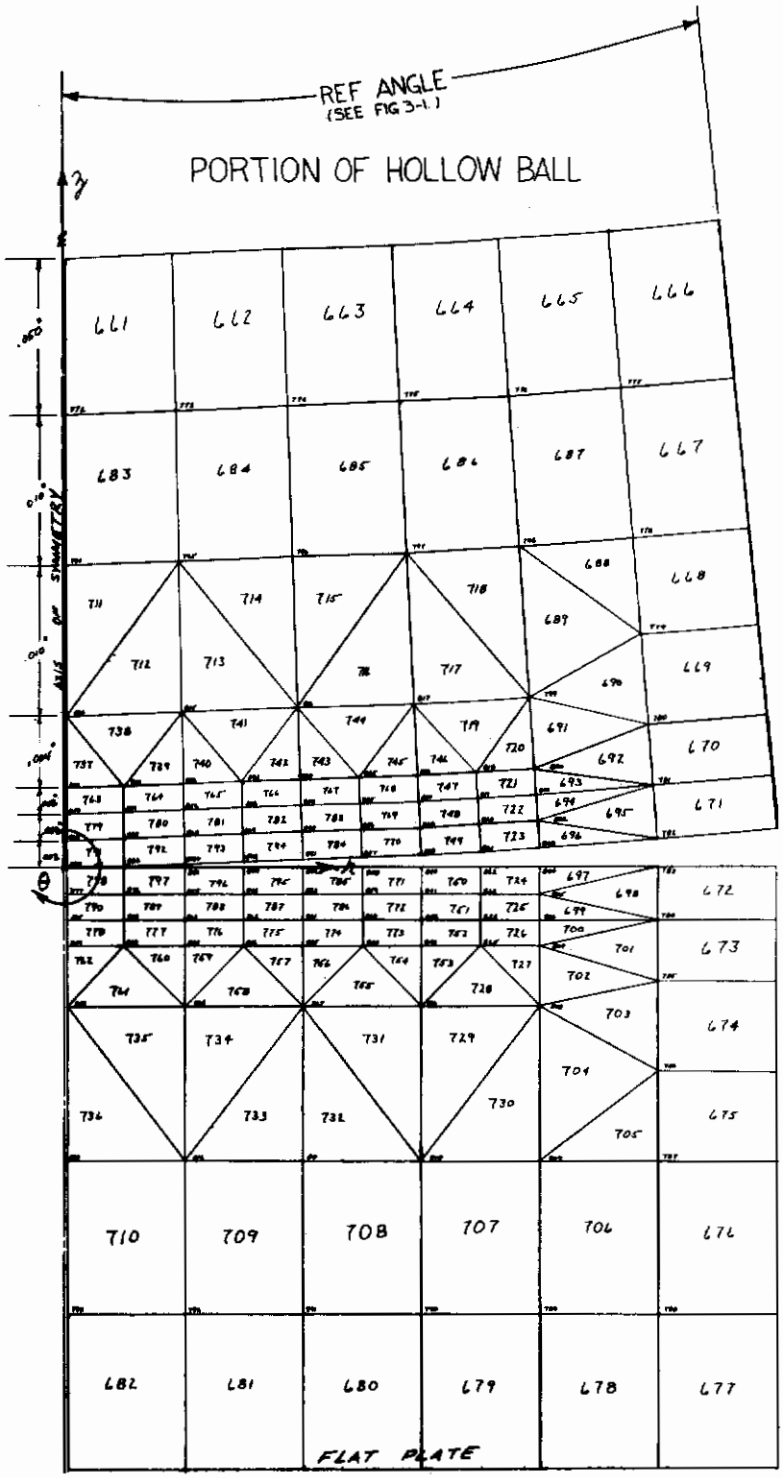

IMPROVED FINITE ELEMENT REPRESENTATION OF HOLLOW BALL IN CONTACT WITH A FLAT PLATE
FLAT PLATE AND A PORTION OF THE BALL ARE SHOWN (SEE FIG. 1 FOR REF.)
883 NODAL POINTS
798 FINITE RING ELEMENTS

Fig. 2 - Model 2 Fine Grid

entire model 2 consists of 798 finite ring elements and 883 nodal points. As each increment of load was added the next two adjacent nodal points (one on the ball and one on the plate) came into contact. The model was then recoded (same number of elements) with one less nodal point (the two points are now considered as one common point). The radius of contact under 1000 pounds load was computed to be 0.0303 inches which brought seven nodal points into common contact and allowed a much more accurate description of the contact surface, contact stresses, and the subsurface contact stress field.

A third mathematical model was unsuccessfully used in an attempt to further define the solution. This third model used a small (23 degrees included angle) segment of the hollow ball with displacement boundary conditions (developed with Model 2) applied to all of the exterior edges. The solution had numerical instabilities and was unsuitable for interpretation of results. The hope was that this final model would result in a single computer-print-out of the total stresses in each element which would have eased the compilation of results.

The results of the Model 2 analysis are described in Section 5. Each of these stresses are the numerical superposition of the individual results of six computer solutions. In general two computer runs were required to obtain each data point. The first run was based upon an estimate of the additional increment of load required to bring the next adjacent nodal points into contact. The second run used the results of the first run to scale a more accurate estimate of the load increment required to just bring the points into common contact. A total of twenty-three computer runs requiring approximately five hours of computer time on a Univac 1107 were required for the analysis discussed in this report.

The coordinate axis system and definition of stress vectors used throughout this report are given in Fig. 3.

The second method of obtaining matching solutions was not attempted.

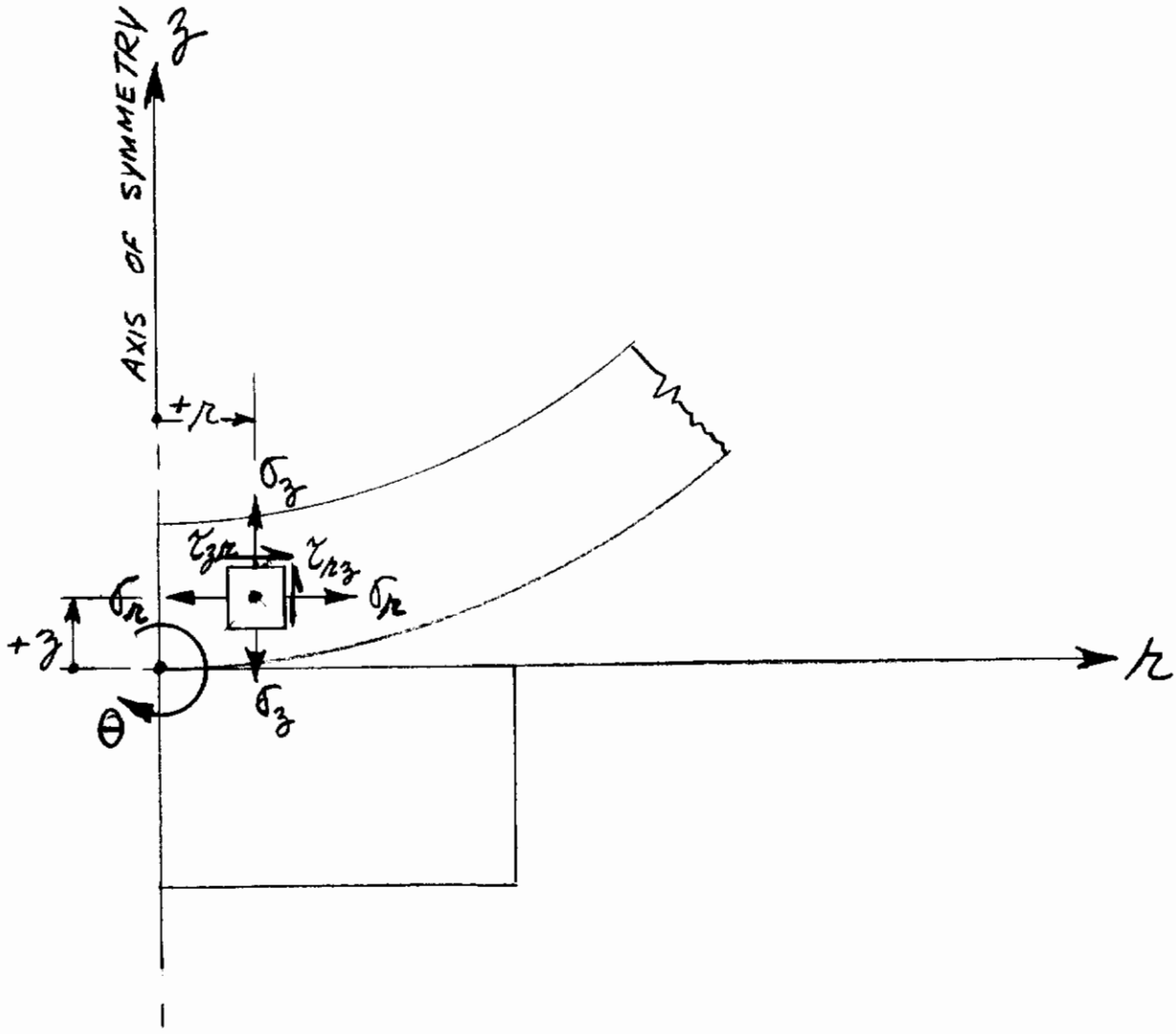

Fig. 3 – Hollow Ball Coordinate Axis System and Stress Representation

SECTION 4

MODEL 1 (COARSE GRID) RESULTS

The results of the analysis of Model 1 are given in Figs. 4, 5, and 6. Fig. 4 depicts the stress distribution along the axis of symmetry for the hollow ball (upper half of graph) and the flat plate (lower half of graph). The σ_z stress is called the Hertz stress at the common surface of contact ($z = 0$). The τ_{45} stress is the maximum static shear stress and may be expressed as:

$$\tau_{45} = 1/2 \left| \sigma_z - \sigma_r \right| \qquad \text{(psi)}$$

The stresses σ_z, σ_r, and σ_θ are principal stresses along the axis of symmetry ($r = 0$).

It is interesting to note that the hollow ball curves are very similar to the flat plate curves with the exception of the σ_r and σ_θ stress at the inside surface of the ball. The maximum stress values of interest are given in Table I.

Table I

MAXIMUM STRESS VALUES FOR MODEL 1

	Hollow Ball	Flat Plate
σ_z max. ($z = 0$)	585,000 psi	585,000 psi
τ_{45} max.	130,000 psi	190,000 psi
Depth to τ_{45} max	0.016 in.	0.014 in.

The magnitude of the maximum unidirectional shear stress (τ_{45}) is less in the hollow ball than in the flat plate. It is reasonable to predict that as the ball wall thickness increases the ball stress curves will approach those of the flat plate. The values of σ_θ and σ_r on the inside surface of the ball will approach zero as the wall thickness increases. The distribution and magnitude of the shear stress (τ_{45}) will become the mirror image of the flat plate for a wall thickness which approaches the radius of the ball. The classical solution of the solid ball on a flat plate, Section 6, has identical solutions for the ball and the plate.

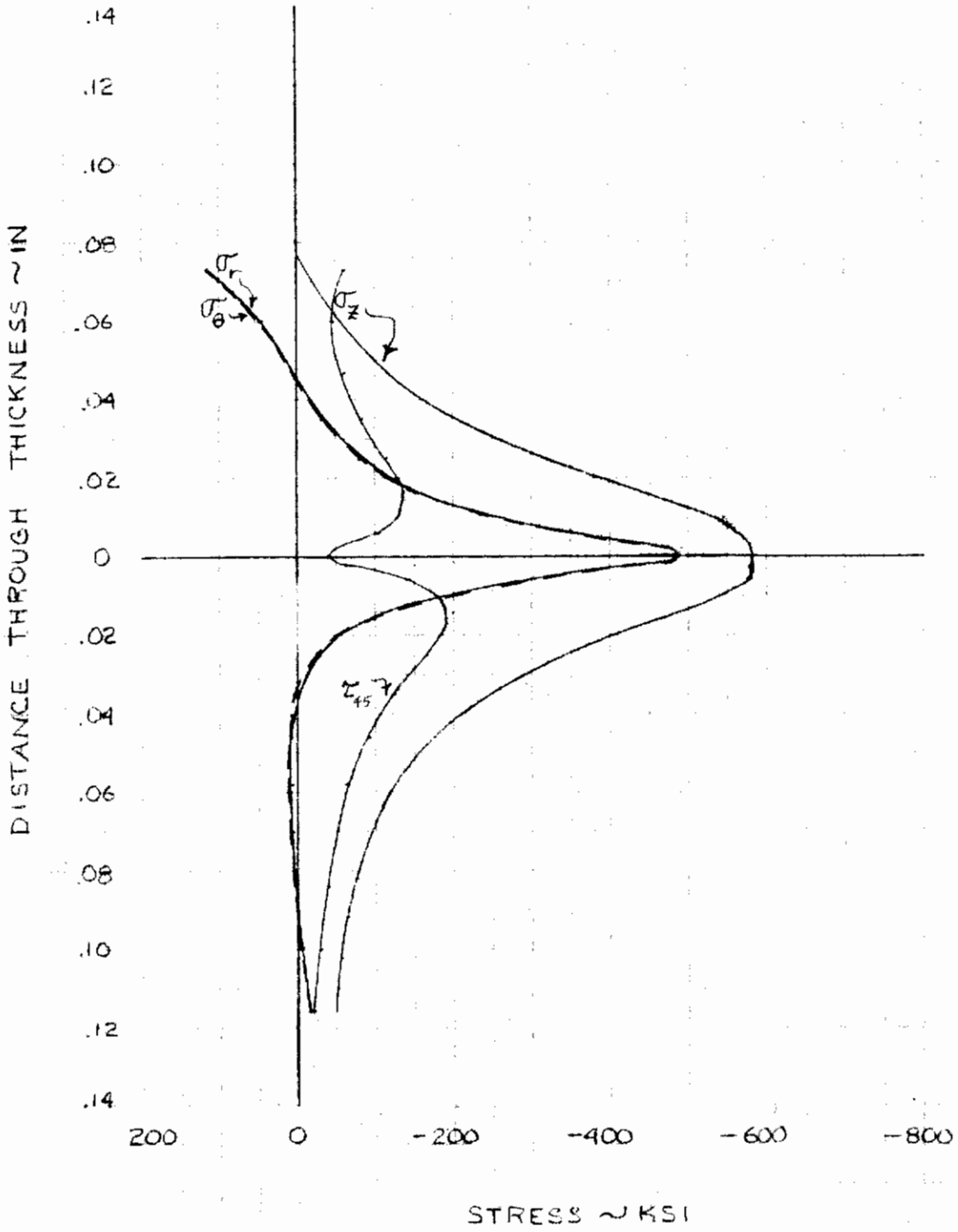

Fig. 4 - Subsurface Stress Plot Along Axis of Symmetry (r = 0) Model 1.

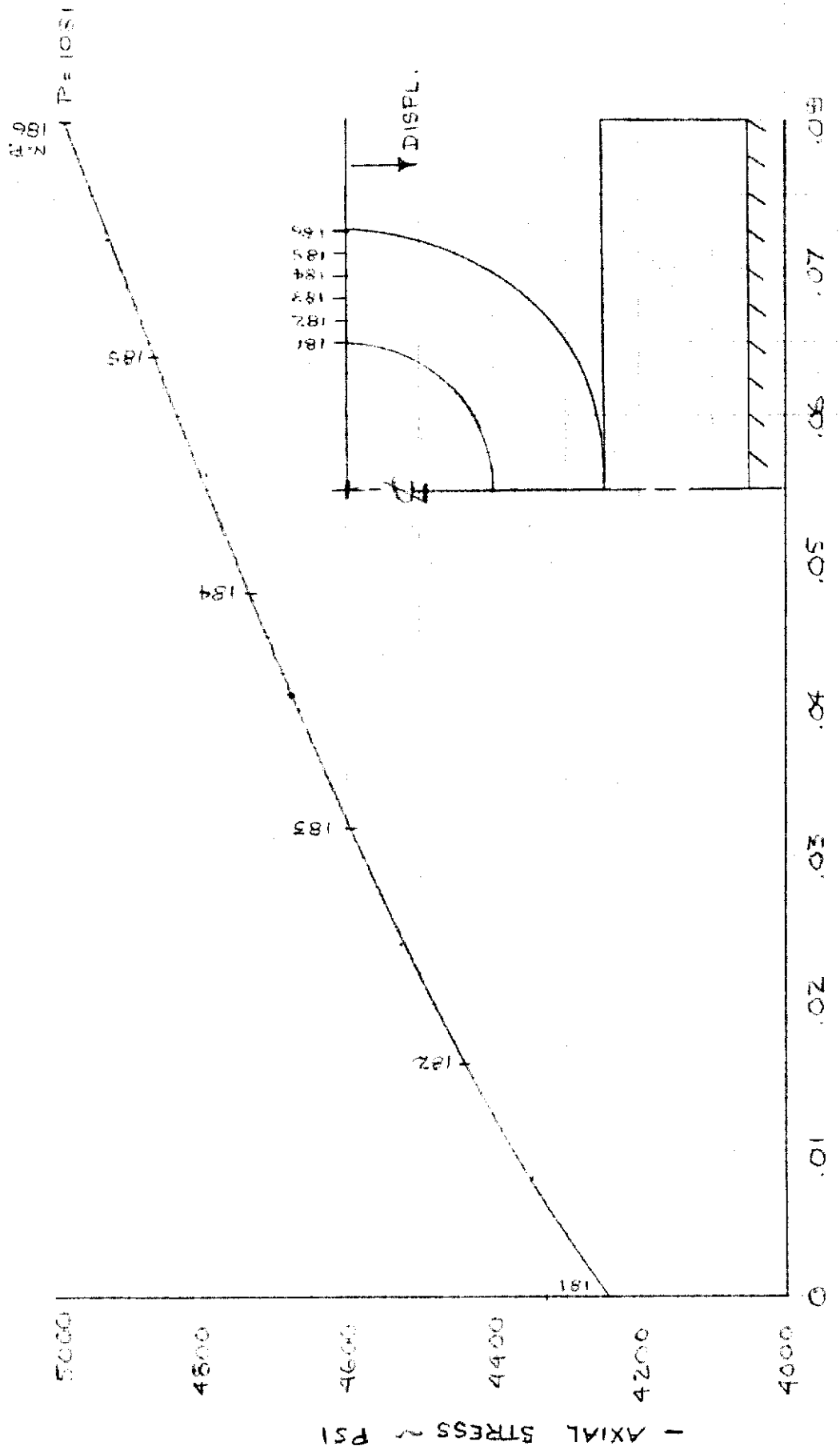

Fig. 5 - Hollow Ball Stress at 90° to Load.

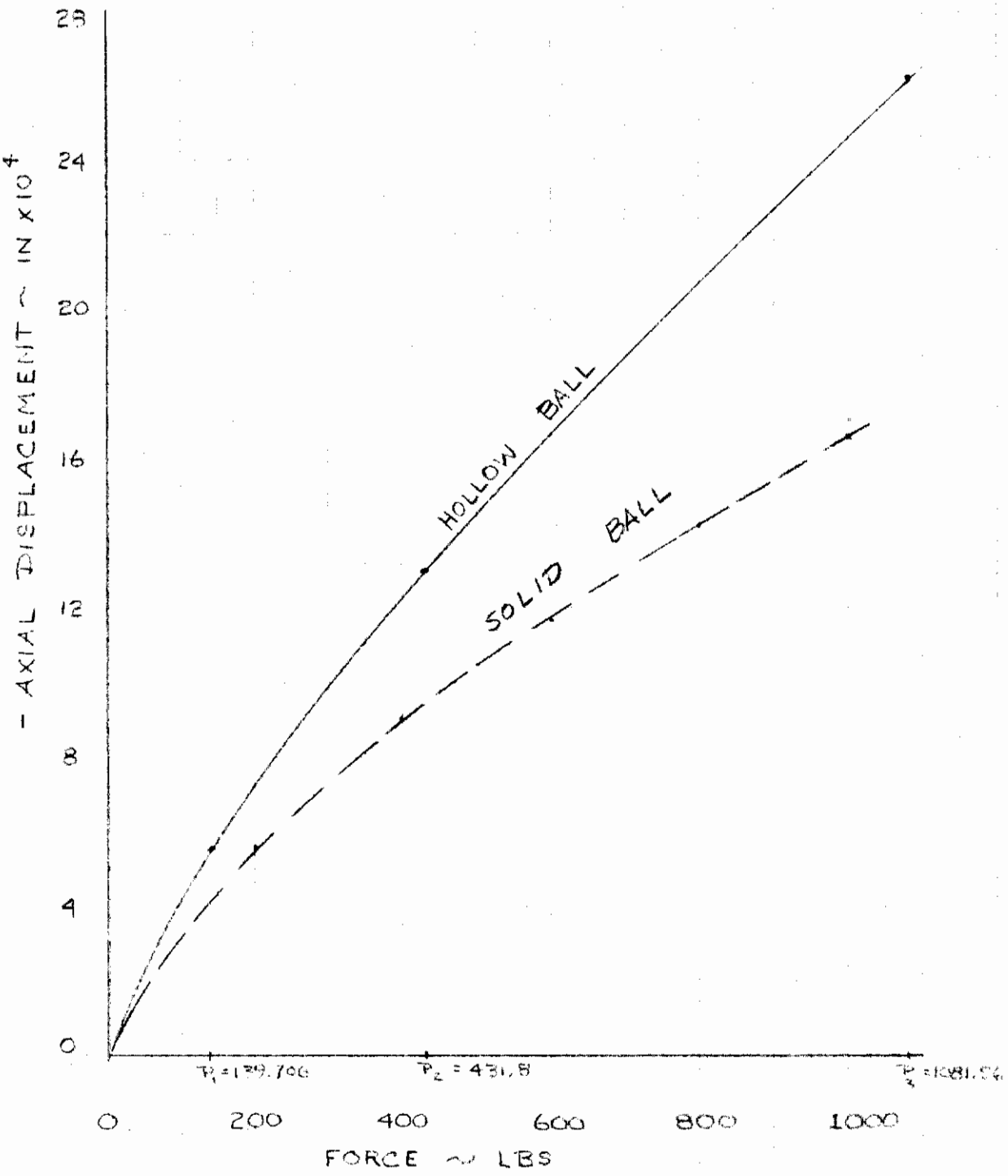

Fig. 6 - Total Elastic Approach of a Hollow Ball in Contact with a Flat Plate.

The stress distribution at the equator of the hollow ball is given in Fig. 4. The stress varies from 4240 psi at the inside surface to 4985 psi at the outer ball surface. The average compressive stress resulting from the 1081 pound applied load is:

$$\sigma_{avg} = \frac{P}{\pi[r^2 - (r-t)^2]} = \frac{1081}{\pi[\overline{0.5}^2 - (0.5 - 0.08)^2]} = 4675 \text{ psi}$$

This average compressive stress correlates well with Fig. 5 as it occurs almost at the mid-thickness of the ball wall where the expected centroidal axis would be located.

The total approach of the center of the one-inch-diameter hollow ball and the flat plate is shown in Fig. 6.

SECTION 5

MODEL 2 (FINE GRID) RESULTS

The finer grid spacing (Fig. 2) of Model 2 resulted in essentially the same stress distribution pattern along the axis of symmetry (r = 0) of the hollow ball (Fig. 7) when compared to the results from Model 1 (Fig. 4). The finer grid spacing did allow for a better description of the entire subsurface stress field.

The normal stresses σ_z, σ_r, and σ_θ are principal stresses only on the axis of symmetry (r = 0). At all other locations the orthogonal shear stress τ_{rz} is of considerable interest. The values of these four stresses are plotted as a function of the radial distance from the axis of symmetry for various axial distances from the contact surface. The finite element type of solution computes average stress values which are located at the centroid of the finite element. The available stress values and the specific graphs are limited to the grid work used for the analysis. (Model 2, Fig. 2). Table II lists the available stress plots and the maximum stress values of interest.

Table II

VALUES AND LOCATION OF MAXIMUM ORTHOGONAL SUBSURFACE SHEAR STRESS

Fig	Axial Distance (z) From Ball Surface (in.)	σ_z max psi	Radial Location In.	τ_{rz} max psi	Radial Location
8	0.001	585,000	0.0042	125,000	0.0224
9	0.003	565,000	0.0040	135,000	0.0224
10	0.005	548,000	0.0040	135,000	0.0220
11	0.00733	500,000	0.0040	155,000	0.0220
12	0.00867	490,000	0.0040	157,000	0.0246
13	0.01333	425,000	0	142,000	0.0232
14	0.01667	405,000	0	118,000	0.0232
15	0.025	300,000	0	100,000	0.0240

Fig. 16 gives the axial and radial displacements in the contact area. These values essentially describe the shape of the contact zone in the flat plate measured from the original flat surface. They are not total displacements c. the center of the ball with respect to the flat plate.

The σ_r, σ_θ, and σ_z stresses are symmetric about the axis of symmetry. The orthogonal shear stress τ_{rz} is also symmetric about the axis of symmetry but a plane section through the ball and plate would show a reversal in sign from $\theta = 0°$ to $\theta = 180°$. This reversing sense of the orthogonal subsurface shear stress is important in terms of relating the

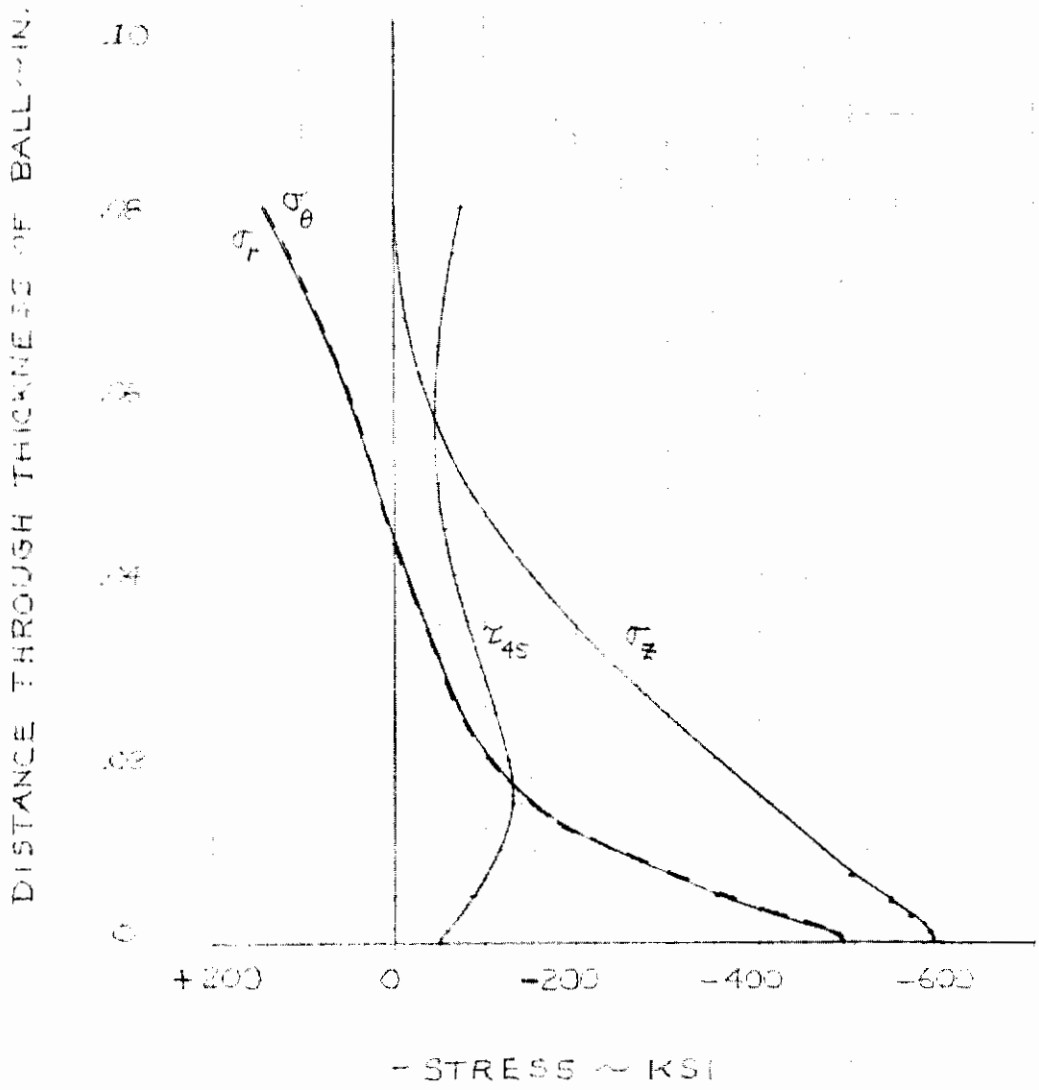

Fig. 7 - Hollow Ball Subsurface Stress Plot Along Axis of Symmetry (r = 0) Model 2.

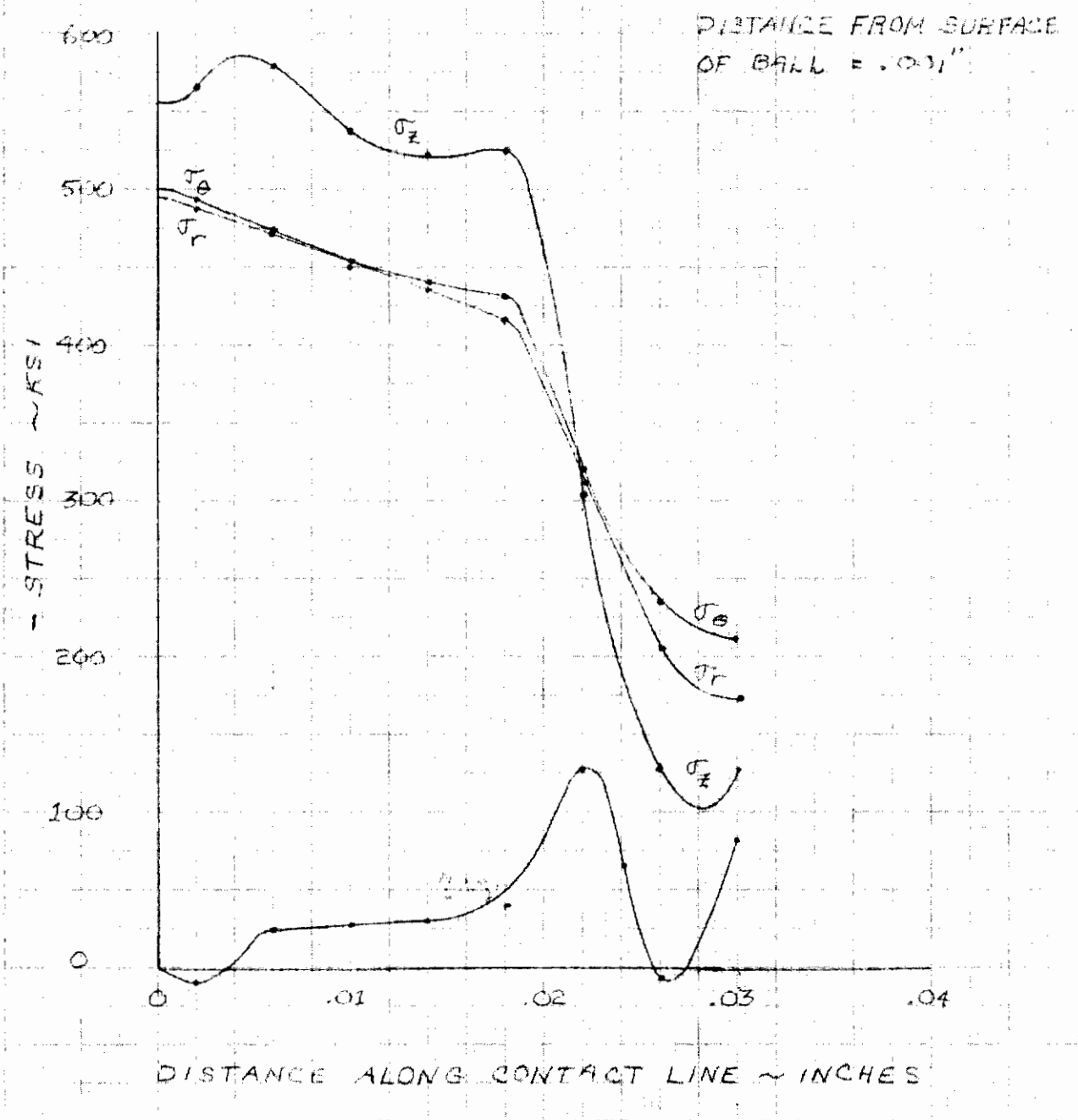

Fig. 8 - Subsurface Stress Plot (z = 0.001").

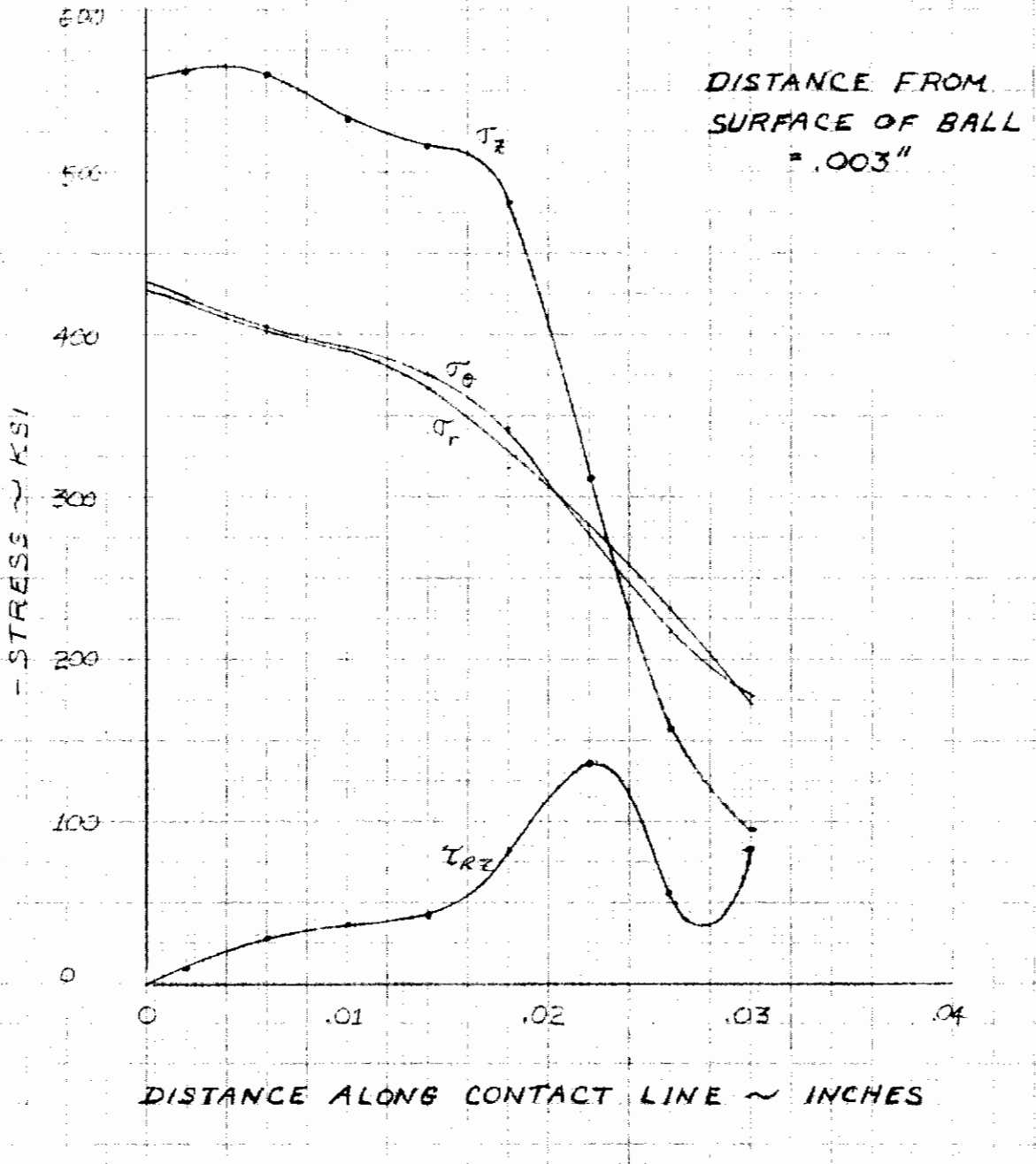

Fig. 9 - Subsurface Stress Plot (z = 0.003").

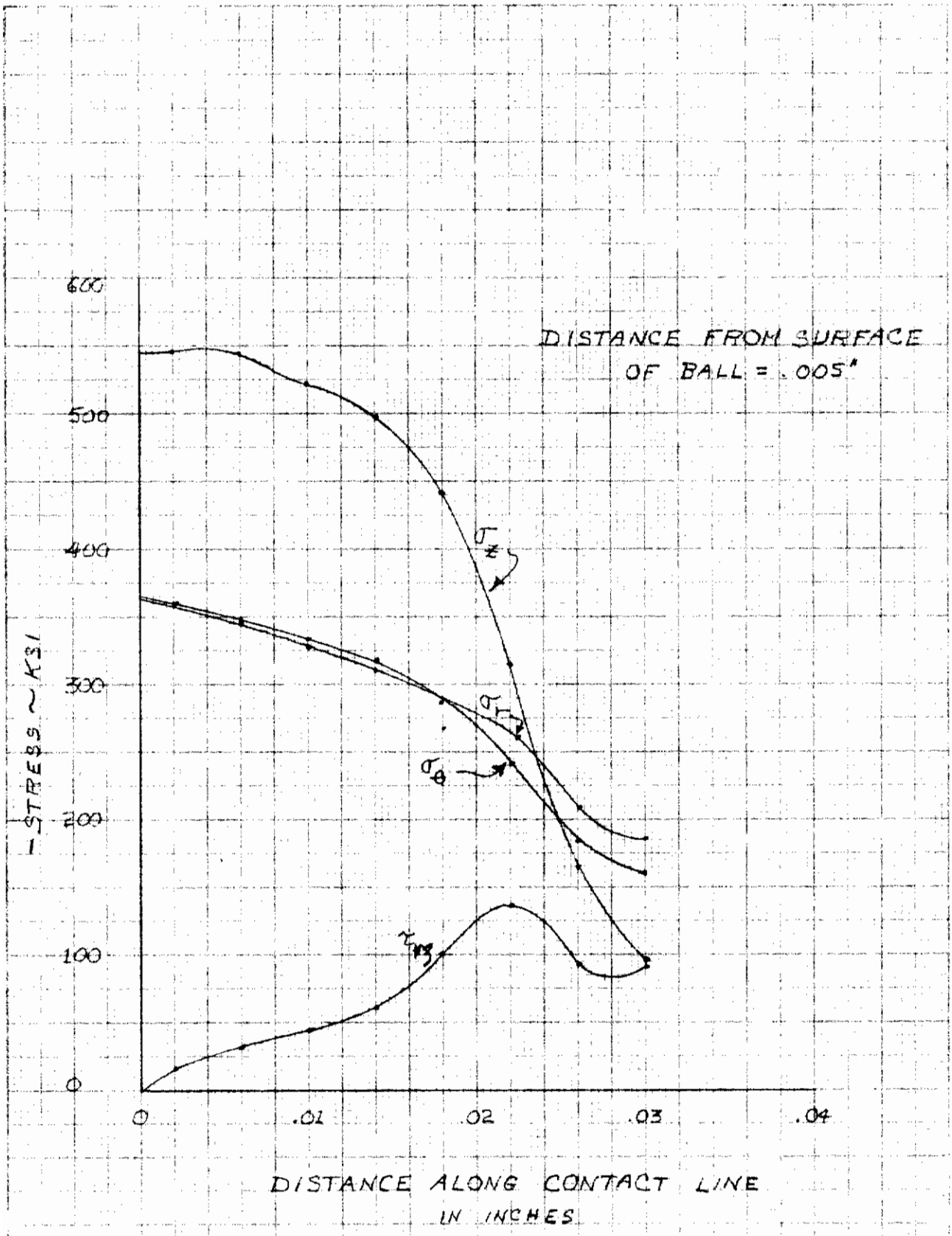

Fig. 10 - Subsurface Stress Plot (z = 0.005").

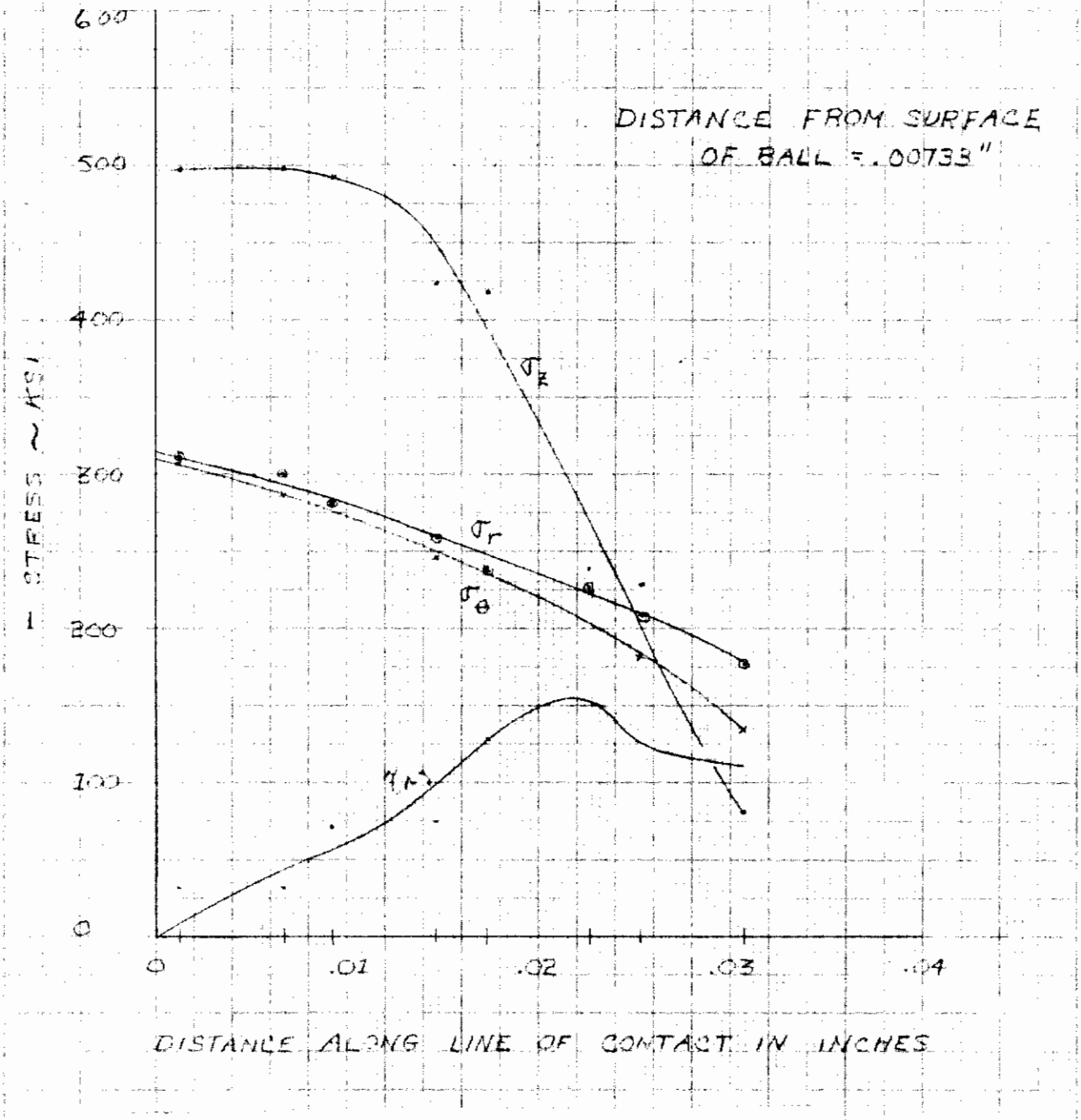

Fig. 11 - Subsurface Stress Plot (z = 0.00733").

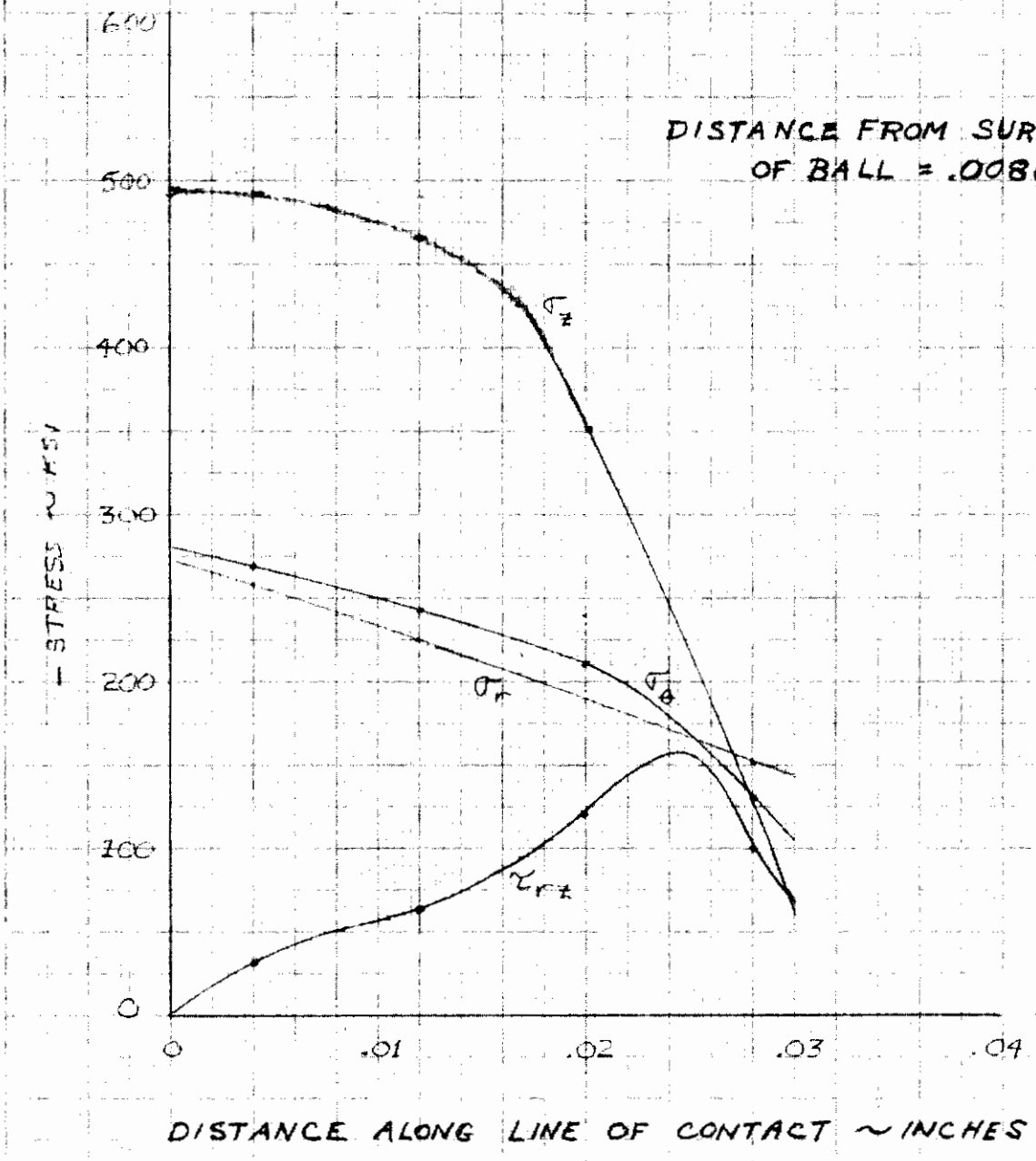

Fig. 12 - Subsurface Stress Plot (z = 0.00867").

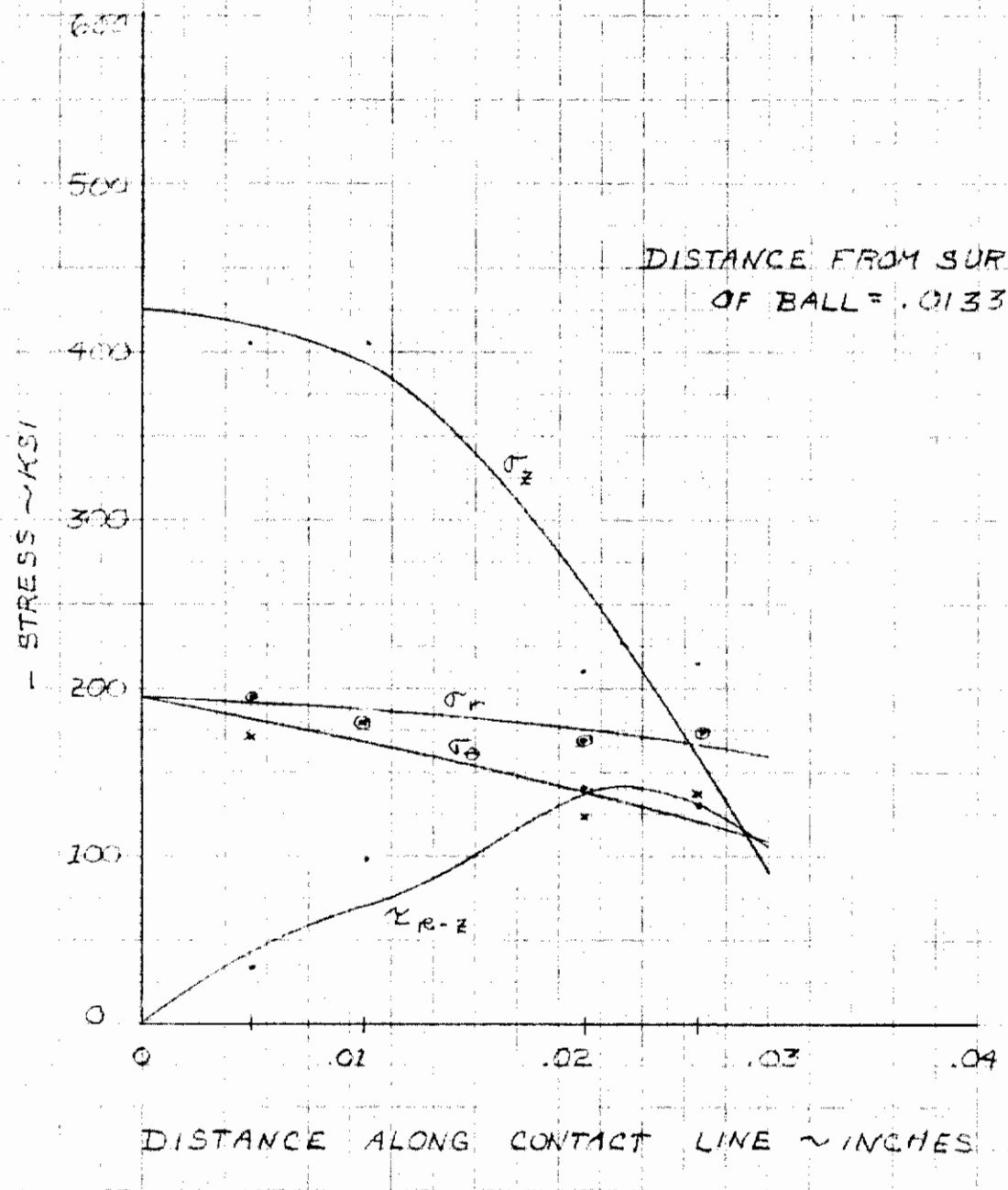

Fig. 13 - Subsurface Stress Plot (z = 0.01333").

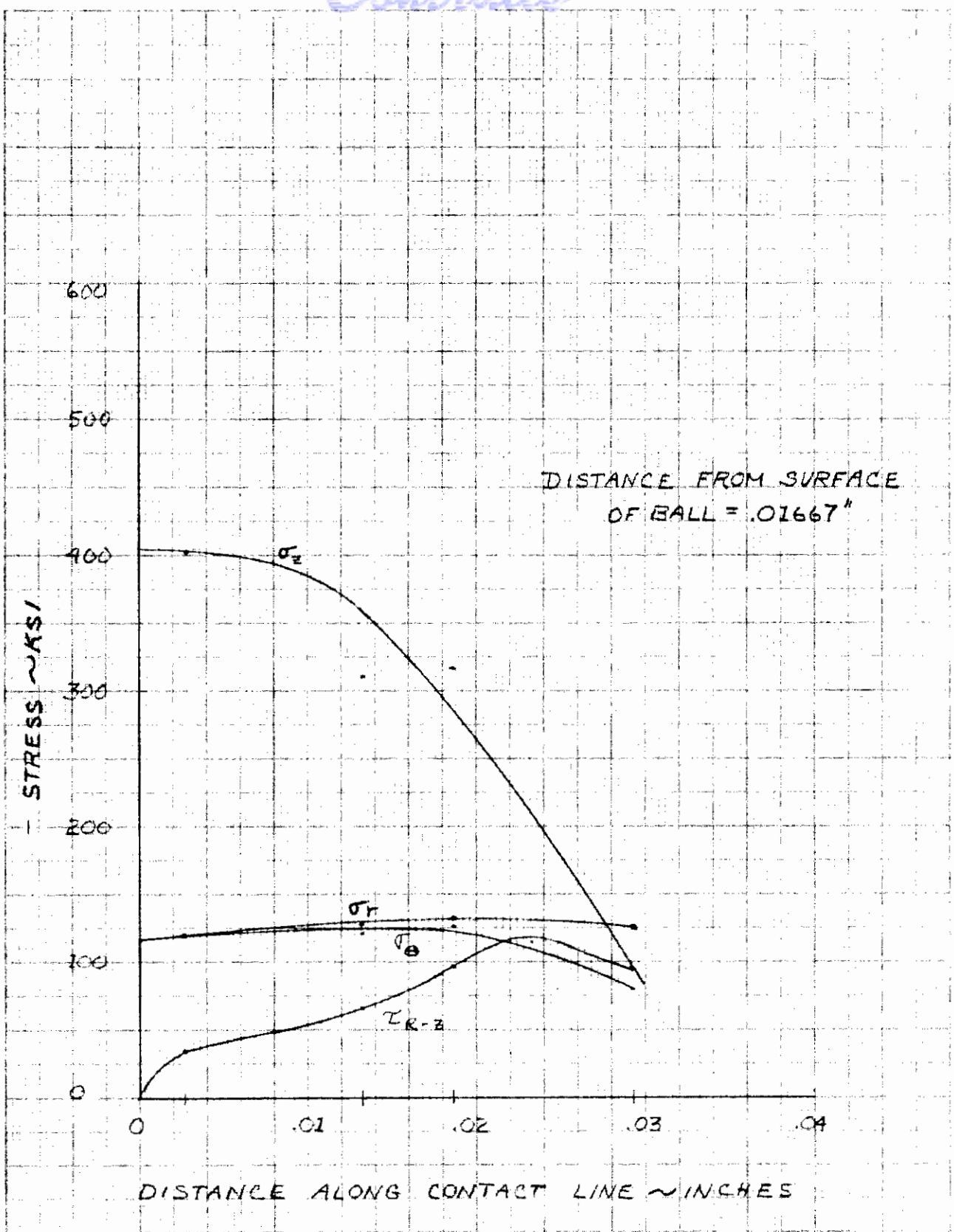

Fig. 14 - Subsurface Stress Plot (z = 0.01667").

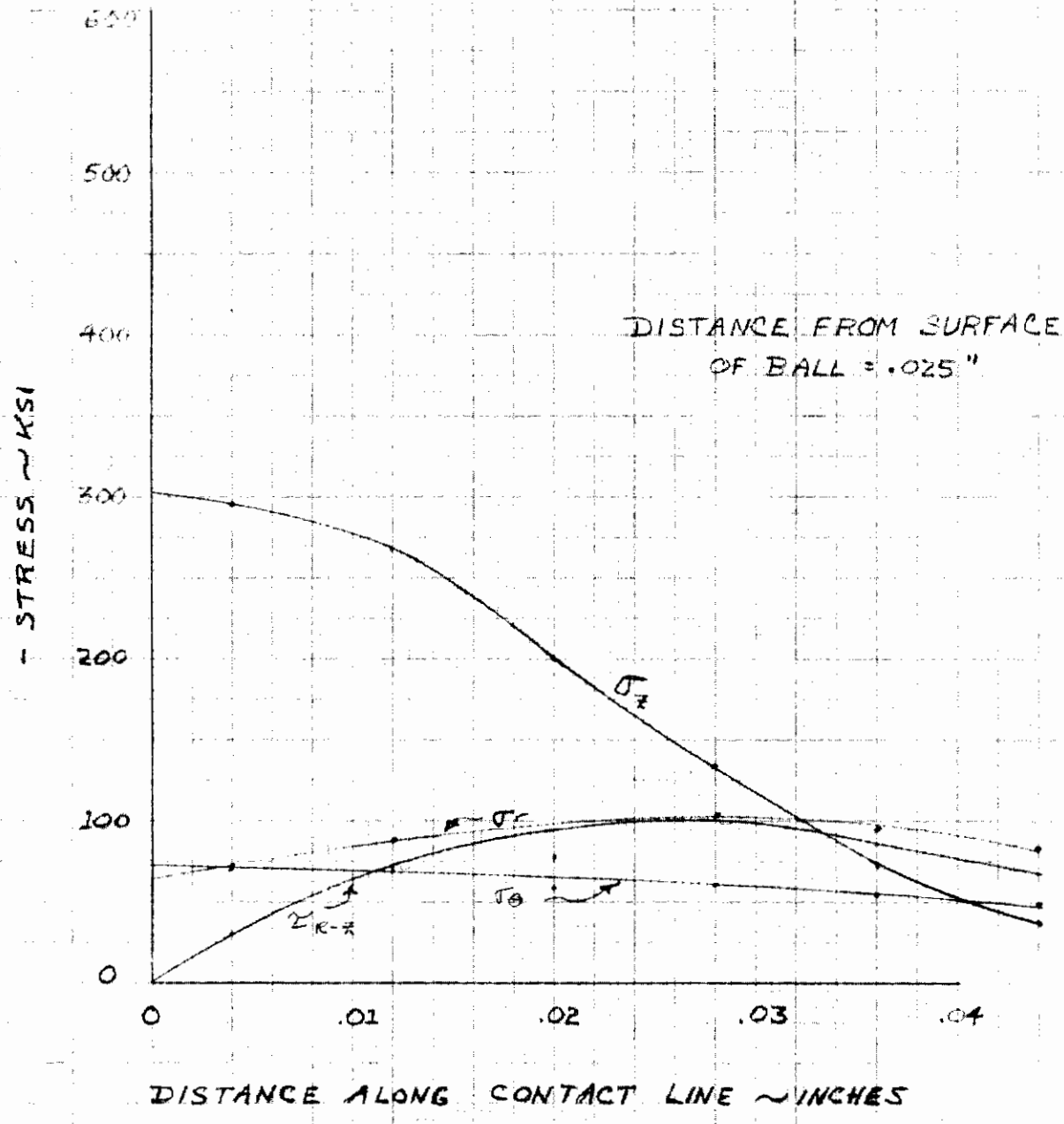

Fig. 15 - Subsurface Stress Plot (z = 0.025").

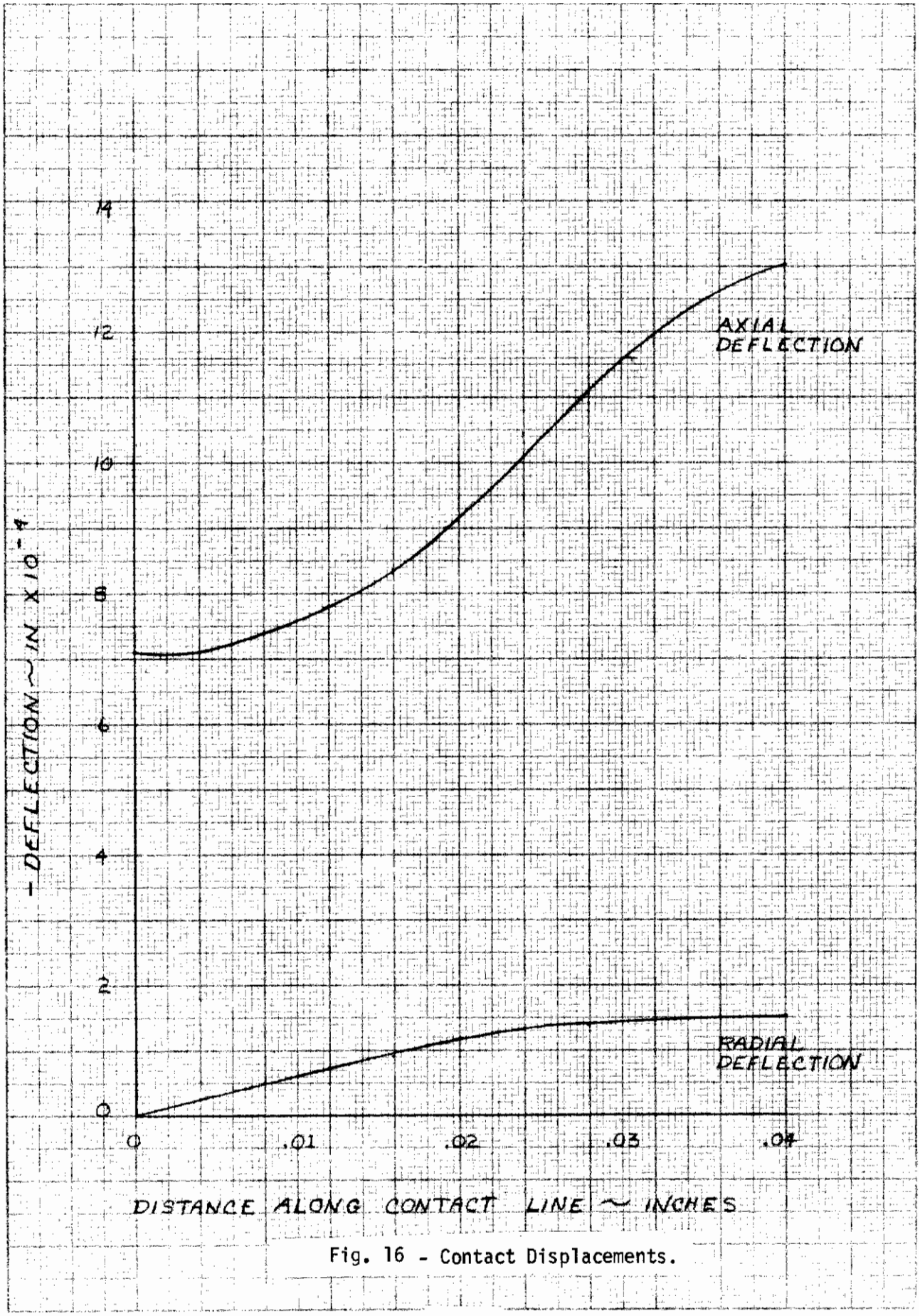

Fig. 16 - Contact Displacements.

stress field to contact stress repetition life estimates. Fig. 17 illustrates the complete subsurface stress pattern at a depth of 0.00733 inches below the contact surface. This subject will be treated in more detail in subsequent sections of this report.

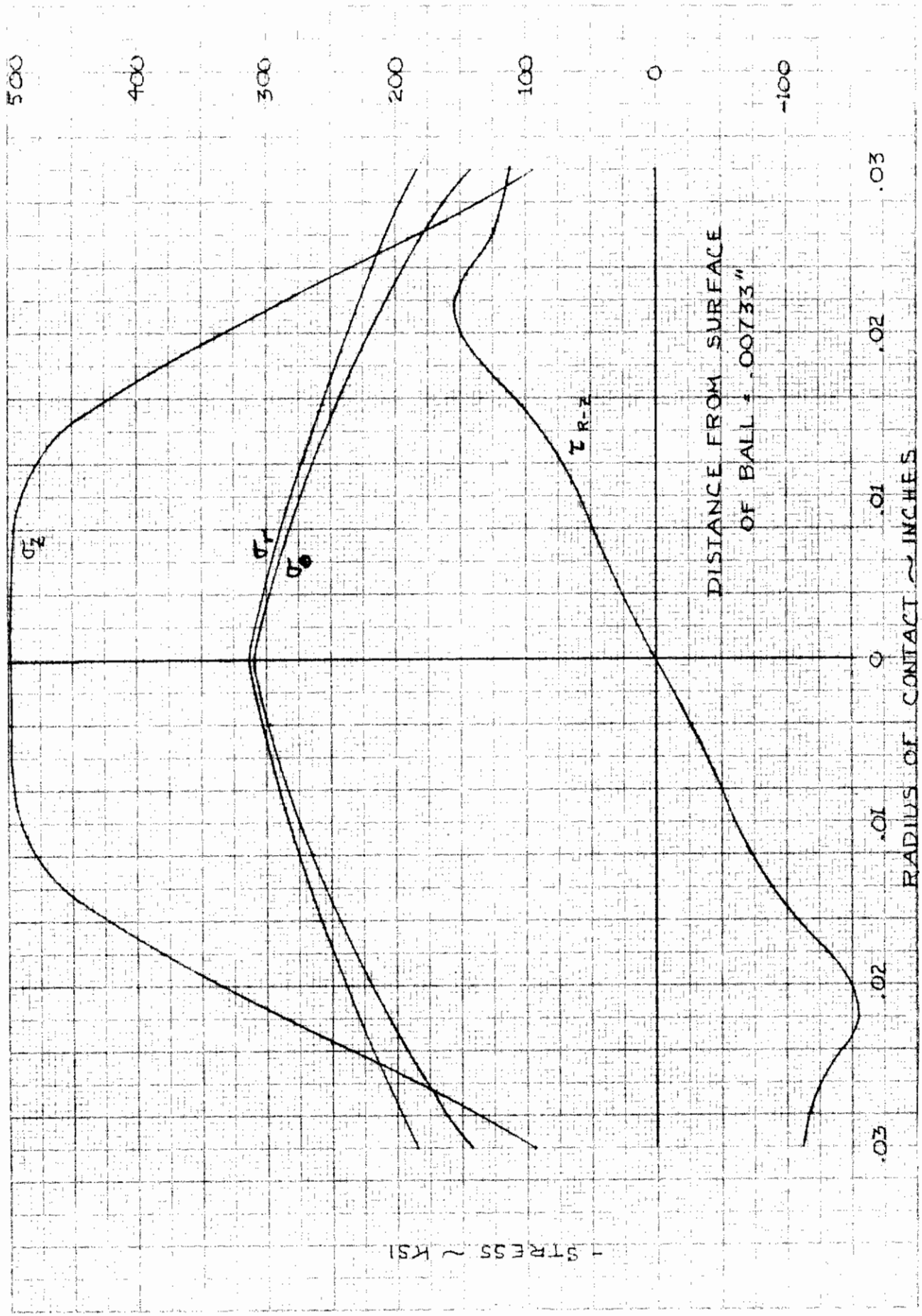

Fig. 17 — Complete Subsurface Stress Plot (z = 0.00733") Illustrating Reversing Orthogonal Subsurfaces Shear Stress, τ_{rz}.

SECTION 6

SOLID BALL ON A FLAT PLATE

The classical analytical solution of the elastic contact of a solid ball on a flat plate has been completely solved by Belyayev (Ref. 5) for the complete stress field in the region of the contact. Verification of the solution has been presented by numerous authors providing that the elastic limit of the materials has not been exceeded. (Ref. 6 & 7). Figure 18 illustrates the type of contact and presents the nomenclature of the variables. Figure 19 illustrates the stress field in terms of an x, y, z rectangular, orthogonal coordinate axis system. Table III gives the formulas used to calculate the parameters of interest. The contact zone is described by a circle of radius "a" for this specific case and the problem is axisymmetric.

Figure 20 illustrates the subsurface stress field and shows the unidirectional subsurface shear stress, τ_{45}, which reaches a maximum along the axis of symmetry running through the center of the contact. This subsurface shear which occurs on a 45° plane is decisive in static calculations or predictions of plastic flow when the elastic limit of the material is exceeded. The magnitude of this unidirectional stress is equal to 32% of the maximum Hertz contact stress. Figure 19 illustrates the location of the maximum subsurface reversing orthogonal shear stress, τ_{zy}. This stress completely reverses from tension to compression as the ball rolls over the plate. The total magnitude of its range is twice its amplitude and amounts to 43% of the maximum Hertz contact stress. It is this stress range which exceeds that of the unidirectional shear stress which is used by Lundberg and Palmgren (Ref. 8) for the calculation of rolling contact fatigue.

The maximum reversing subsurface orthogonal shear stress shown in Figure 19 is located at a depth below the contact of 35% of the radius of the elastic contact and at a radius of 85% of the elastic contact radius from the axis of symmetry.

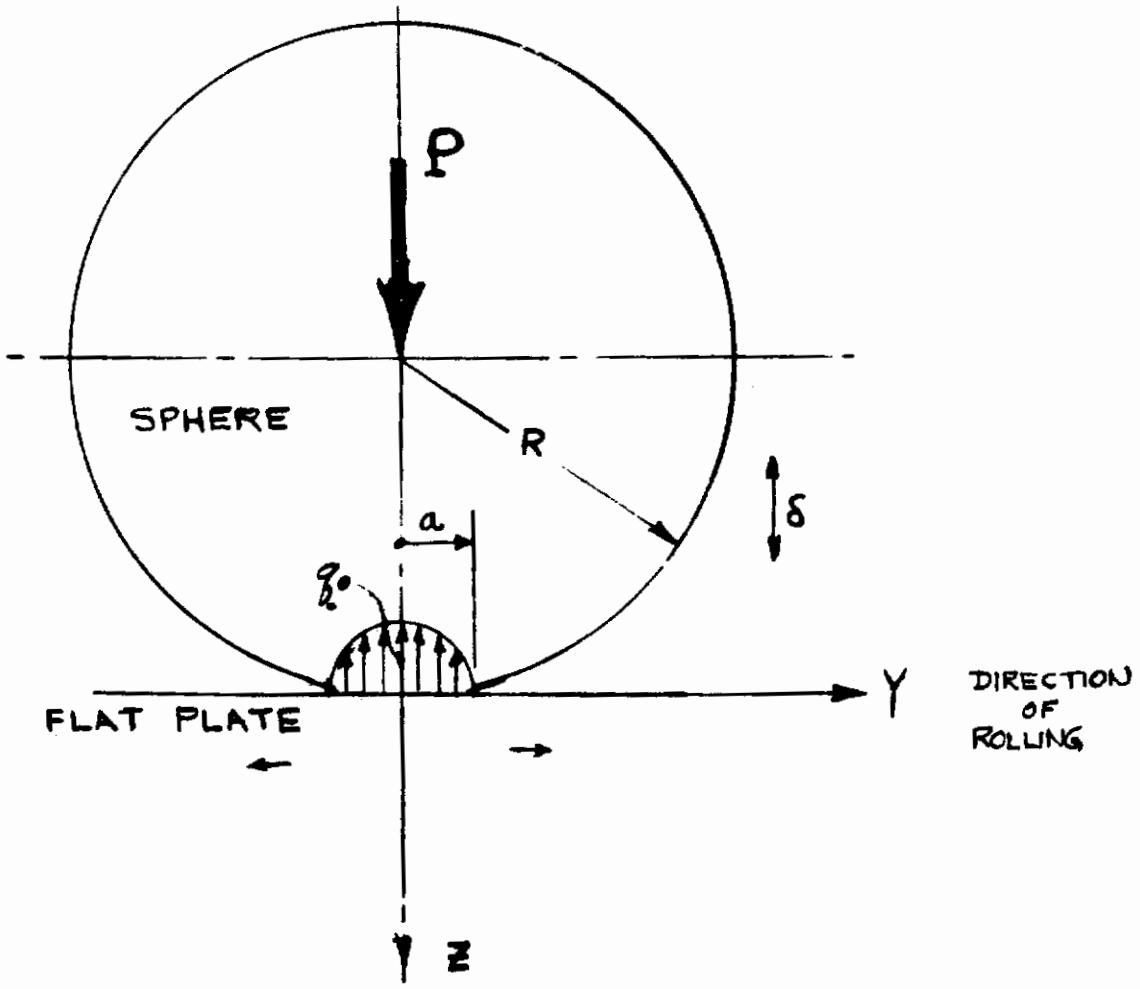

P = Applied Load (Lb.)
R = Radius of Sphere (in)
a = Radius of Elastic Contact Area (in.)
q = Hertz Compressive Contact Stress (psi)
q_o = Max. Hertz Stress (psi)
δ = Approach of Sphere and Plate (in.)

Fig. 18 - Elastic Contact of a Solid Ball and a Flat Plate

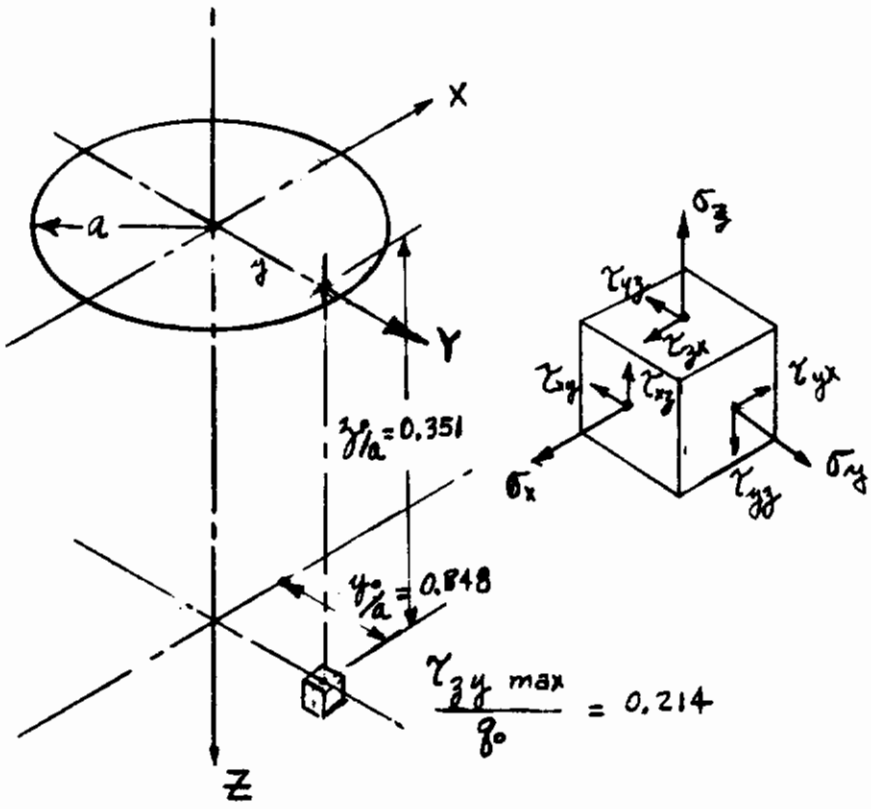

Fig. 19 - The Stress Field Showing Location of Maximum Subsurface Reversing Orthogonal Shear Stress, τ_{zy}, Decisive for Fatigue

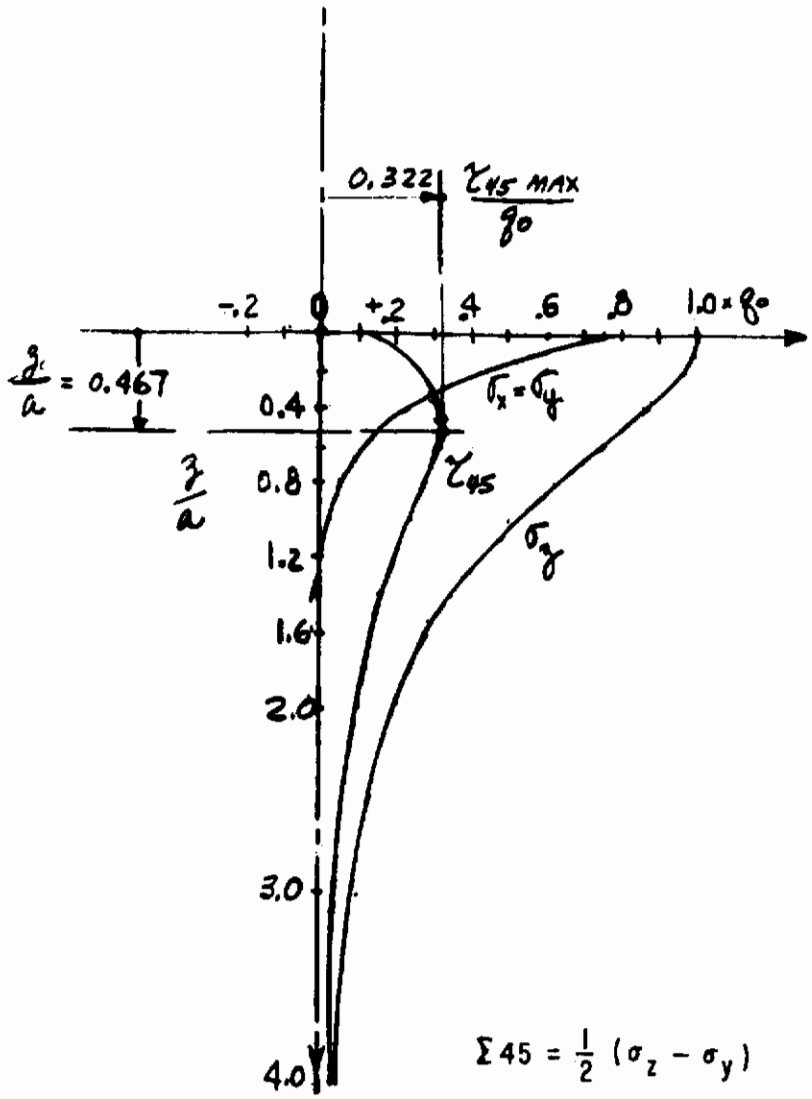

DIRECTLY BELOW THE CENTER OF CONTACT (x=y=0) SHOWING LOCATION OF MAXIMUM UNIDIRECTIONAL SUBSURFACE SHEAR STRESS, τ_{45}, DECISIVE FOR STATIC LOADING.

Fig. 20 - Subsurface Stress Field

Table III

FORMULAS FOR ELASTIC CONTACT OF A SOLID BALL AND A FLAT PLATE

Symbol	Description	Formula	Specific Values
a	Radius of Elastic Contact Area (in.)	$a = 0.00361\,[PR]^{1/3}$	(1) 0.0287 in.
δ	Approach of Sphere and Plate (in.)	$\delta = 0.131 \times 10^{-4} \frac{P^{2/3}}{R^{1/3}}$	(2) 0.001650 in.
q	Hertz Compressive Contact Stress (psi)	$q = \frac{3P}{2\pi a^2} \left(1 - \frac{y^2}{a^2}\right)$	(3) $20.2 \times 10^6 \quad (.0287)^2 - y^2$
q_o	Maximum Hertz Stress (psi)	$q_o = \frac{3.65 \times 10^4 \, P^{1/3}}{R^{2/3}}$	(4) 579,400 psi
τ_{45}	Maximum Unidirectional Subsurface Shear Stress (psi)	$\tau_{45} = 0.322\, q_o$	(5) 186,567 psi
z_{45}	Depth to τ_{45} ($x = y = 0$) (in.)	$z_{45} = 0.467\, a$	(6) 0.0134 in
τ_{zy}	Maximum Reversing Orthogonal Sub surface Shear Stress (psi) (single amplitude)	$\tau_{zy} = \pm 0.214\, q_o$	(7) 123,992 psi
z_o	Depth to Orthogonal Shear (in.)	$z_o = 0.351\, a$	(8) 0.0101 in.
y_o	Radius to Orthogonal Shear (in.)	$y_o = \pm 0.848\, a$	(9) 0.0243 in.

Poisson's ratio = 0.3

Modulus of elasticity = 29×10^6 psi (hard steel R_c 60-62)

P = 1000 lbs.

R = 0.5 inch.

SECTION 7

COMPARISON OF HOLLOW BALL AND SOLID BALL STRESS FIELDS

The subsurface stresses along the axis of symmetry (r = 0) are plotted in Fig. 21 for the one-inch diameter hollow ball (wall thickness = 0.080 inches) and a solid ball contact with a flat plate. The normal stress, σ_z, is approximately the same at the contact surface (z = 0) (Hertz contact stress) for both contacts.

The normal stress is less in magnitude for the hollow ball contact throughout the subsurface. The radial stress, σ_r, and the hoop or circumferential stress, σ_θ, are identical for this axisymmetric case and are compared to the σ_x radial stress values from solid ball theory. The hollow ball stresses (σ_r and σ_θ) result in tensile stresses at the inner ball surface due to bending of the hollow ball. These tensile stress are appreciable and reach 150,000 p.s.i. under 1000 pounds normal ball loading. The hollow ball radial stresses in the compressive stress region ($0 \leq z \leq 0.045$) are less than those for the solid ball contact.

The static, unidirectional, subsurface shear stress, τ_{45}, is significantly lower for the hollow ball stresses.

The Hertz contact stress, σ_z at z = 0, is approximated by the average normal stress at the centroid of the finite elements along the surface of contact. Fig. 22 shows the Hertz contact stress (σ_z at z = 0.001 inch) for the hollow ball and solid ball contacts. The maximum value of the Hertz contact stress is almost the same for both cases. The hollow ball shows some stress relief at the center of the contact due to bending effects in the spherical shell. The hollow ball contact deformations, which define the shape of the deformed contact surface are also shown in Fig. 22. Note the fact that the radius of contact is greater for the hollow ball contact.

The orthogonal, reversing, subsurface shear stress, τ_{rz}, is described in Section 5 (Figs. 8 through 15) for the hollow ball contact. The maximum values of τ_{rz} at the various depths (z) occur at radial distances of $0.022 \leq y \leq 0.025$ in. Fig. 23 shows a plot of these maximum values and locates the maximum τ_{rz} value of 160,000 psi for the hollow ball contact at z = 0.0096 inches and y = 0.0235 inches for the hollow ball. The corresponding shear stress for the solid ball contact at this location is only 110,282 psi.

Table IV lists numerical values for the comparative data in both dimensional and dimensionless ratio form for the hollow ball and solid ball contacts. The maximum orthogonal, reversing, subsurface shear stress, τ_{rz}, for the hollow ball is greater in magnitude and closer to the surface of contact than the corresponding values for the solid ball contact.

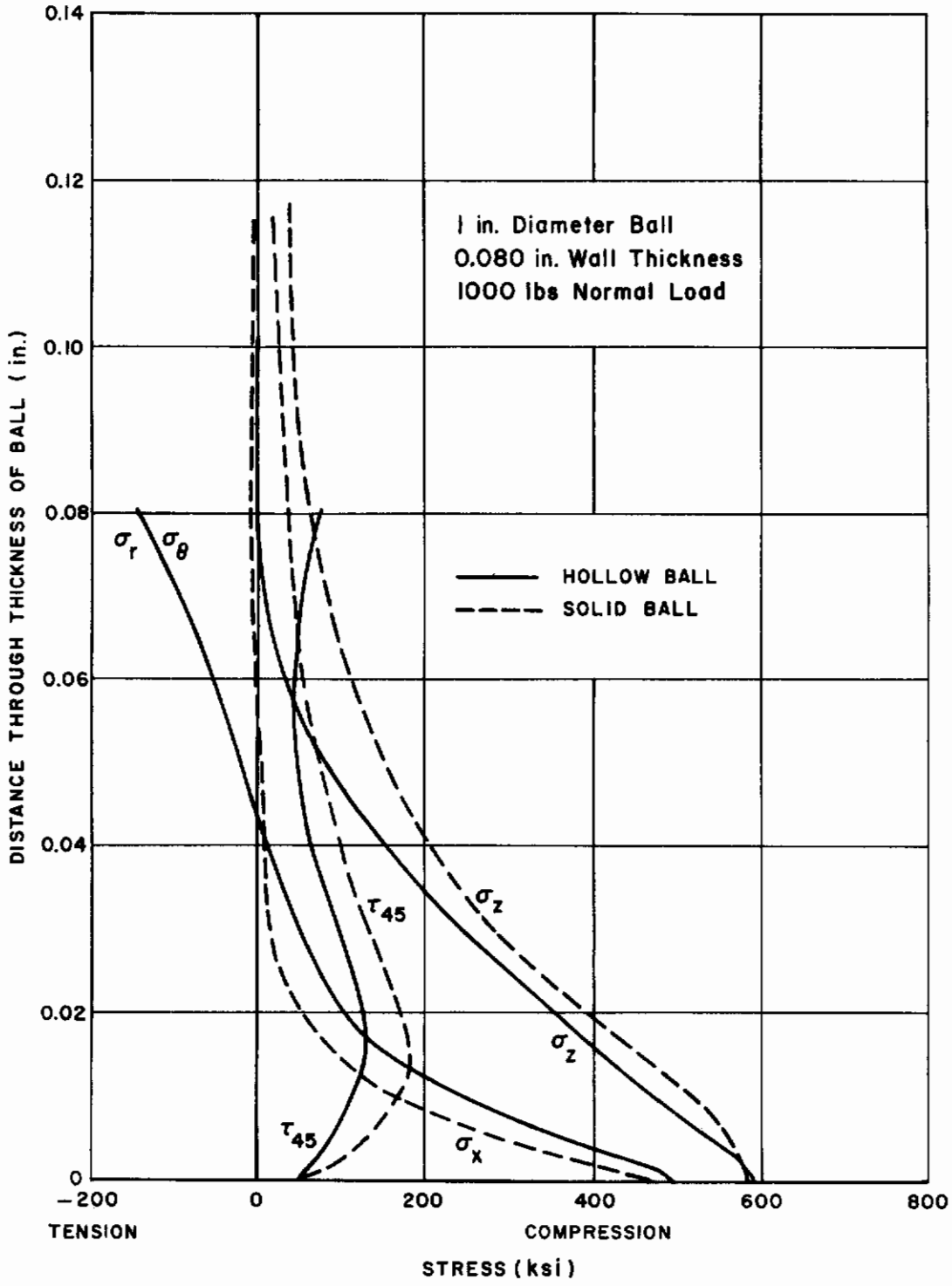

Fig. 21 – Comparison of Hollow Ball and Solid Ball Subsurface Stress Along Axis of Symmetry

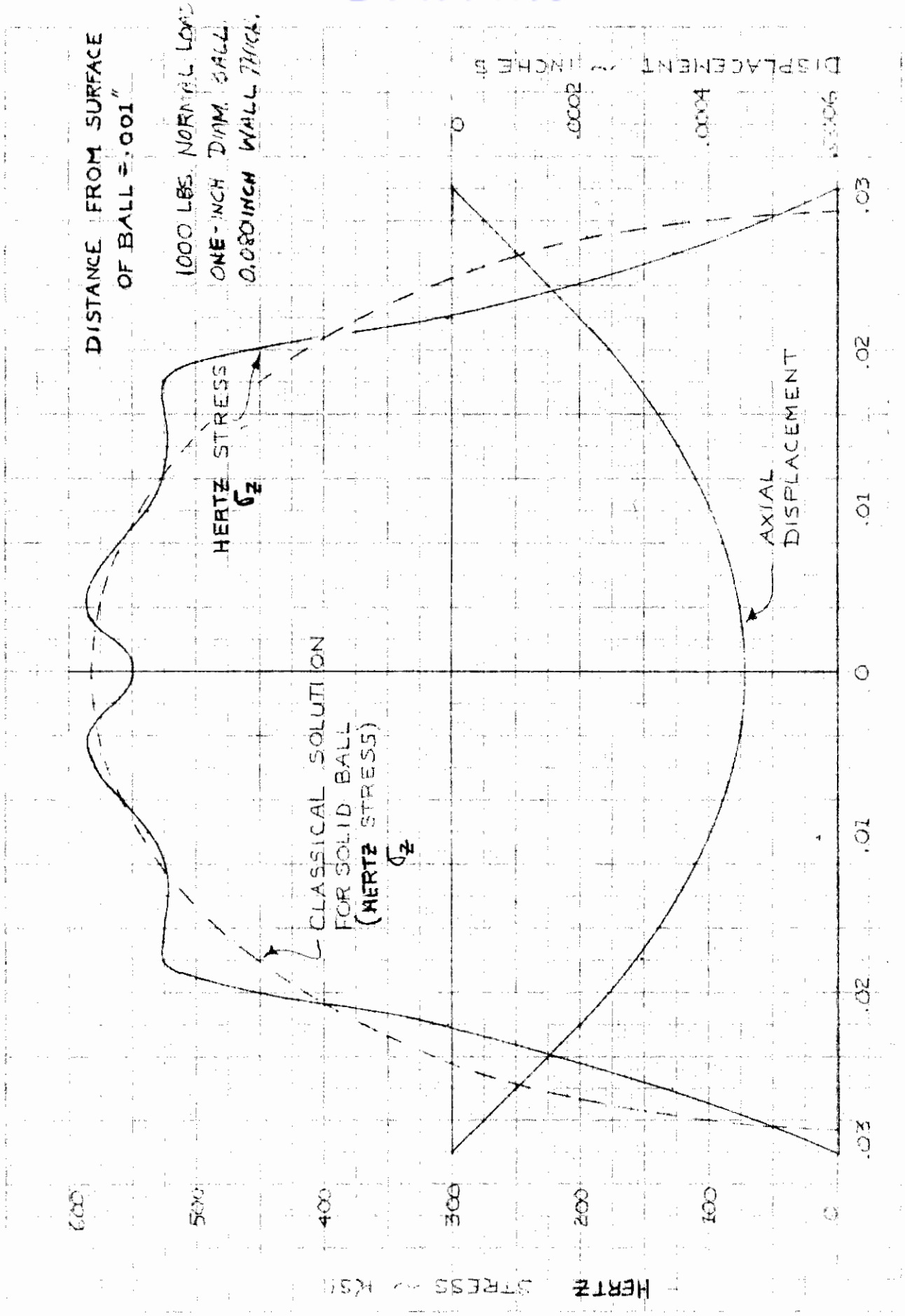

Fig. 22 – Comparison of Hollow Ball and Solid Ball Surface (HERTZ) Contact Stresses

σ_z max = 585,000 PSI

a = 0.0303" CONTACT RADIUS

$\frac{\tau_{RZ\ max}}{\sigma_z} = \frac{160{,}000}{585{,}000} = 0.274$

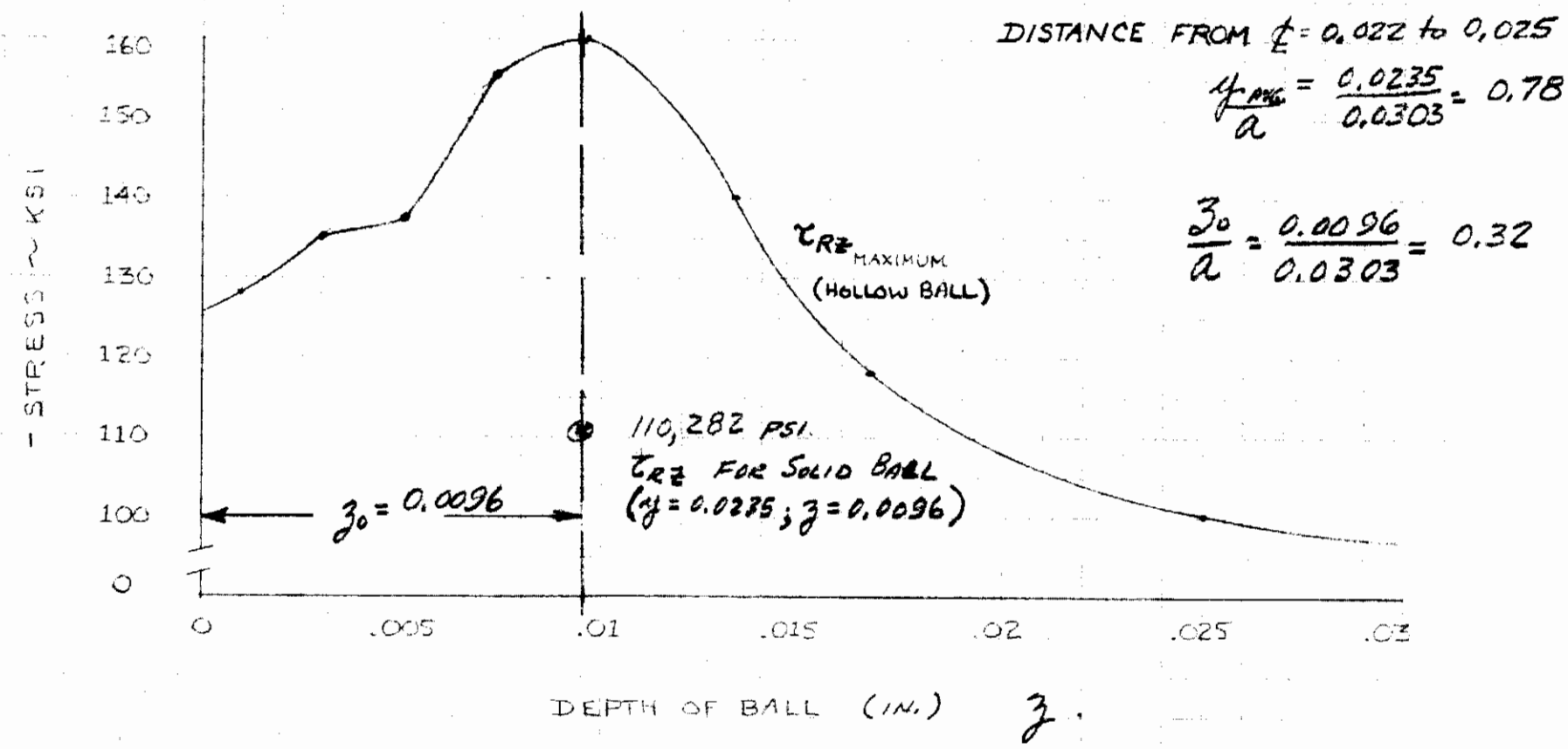

MAXIMUM VALUES OF ORTHOGONAL, REVERSING, SUB-SURFACE SHEAR

Fig. 23 - Maximum Values of Orthogonal Reversing Subsurface Shear Stress in Hollow Ball.

Table IV

COMPARATIVE DATA FOR CONTACT OF ONE-INCH DIAM. BALL AND FLAT PLATE

Item	Symbol	Units	Hollow Ball 0.080 inch Wall	Solid Ball
Contact Radius	a	in.	0.0303	0.0287
Hertz Contact Stress	σ_z	psi	585,000	579,400
Max Unidirectional Static Shear Stress	τ_{45}	psi	130,000	186,567
Depth to Static Shear	z_{45}	in.	0.0160	0.0134
Max. Reversing Orthogonal Shear Stress	τ_{rz}, τ_{zy}	psi	160,000	123,992
Depth to Orth Shear	z_{rz}, z_{zy}	in.	0.0096	0.0101
Radial Dist. to Orth Shear	y_{rz}, y_{zy}	in.	0.0235	0.0243
	τ_{45}/σ_z		0.222	0.322
	z_{45}/a		0.528	0.467
	τ_{rz}/σ_z		0.274	0.214
	z_{rz}/a		0.317	0.351
	y_{rz}/a		0.776	0.848

A comparison of the total approach along the axis of symmetry of the center of the ball with respect to the flat plate for both the one-inch diameter hollow ball (0.080 inch wall thickness) and the one-inch diameter solid ball is shown in Fig. 6 of Section 4. The hollow ball deflects more under the same normal load.

SECTION 8

EXPERIMENTAL VERIFICATION OF RADIUS OF CONTACT

A simple experiment was conducted to check the radius of contact of a one-inch diameter hardened hollow ball with 0.080 inch thick wall in contact with a flat hardened steel plate. Three hollow balls were supplied by the Air Force Flight Dynamics Laboratory, Wright-Patterson Air Force Base.

The hollow balls were placed in contact with a hardened steel (Rockwell C60) flat plate. The plate was coated with a thin layer of copper-sulphate which resulted in a copper colored surface. The ball and plate were placed in an Instron Testing Machine and slowly loaded with a 1000 pound normal load. A burnished or shiny area of contact was evident in the copper coating upon removal of the ball. This observable area was the circle of elastic contact under load. This technique has obten been used successfully to etch the elastic contacts of rollers and balls under load. It is a common practice to etch the exposed copper-sulfate (with the ball in contact) with hydrogen sulphide gas. This objectionable process was not required in this instance. The diameter of the contact circle was measured with a travelling microscope with micrometer adjustment. Table V gives the experimental readings for two test contacts with three readings per contact.

The average contact radius by test was 0.0297 inch which is only 1-1/2% less (0.0006 inches) than the computer contact radius of 0.0303 inch. The experimental compression test provides good experimental correlation with the computer contact radius.

Table V

HOLLOW BALL ELASTIC CONTACT RADIUS
EXPERIMENTAL DATA

ONE-INCH DIAMETER HOLLOW STEEL BALL
(0.08 inch THICK WALL) IN CONTACT WITH A FLAT PLATE UNDER 1000 lbs. NORMAL LOAD

	Beginning Reading (in.)	Final Reading (in.)	Contact Diam. (in.)
Ball #1			
Reading 1	0.3286	0.2689	0.0597
2	0.3371	0.2762	0.0609
3	0.3382	0.2768	0.0614
Ball #2			
Reading 4	0.3352	0.2776	0.0576
5	0.2765	0.2186	0.0579
6	0.3231	0.2649	0.0582

AVERAGE DIAM. = 0.0593 in.

AVERAGE CONTACT RADIUS = 0.0297 in.

SECTION 9

DYNAMIC FATIGUE LIFE ESTIMATE

The presently accepted theory for computing the dynamic fatigue life of rolling bearings (Ref. 8) uses the orthogonal, reversing subsurface shear stress as the decisive stress for the computation of spalling fatigue life. This Lundberg-Palmgren theory forms the basis for the Anti-Friction Bearing Manufacturers (AFBMA) Load Rating Standards for ball and roller bearings.

The life formula for rolling bearings is expressed in Ref. 8 as:

$$\log \frac{1}{S} \sim \frac{\tau_{rz}^{c} N^{e} a\ell}{z_o^{h-1}}$$

S = the probability that the material will survive for N million stress cycles

τ_{rz} = the decisive stress amplitude (psi)

N = millions of stress cycles

a = radius of elastic contact (in.)

1 = length of the raceway (in.)

z_o = depth to decisive stress amplitude (in.)

The exponents, c, h, and e were experimentally correlated with rolling bearing fatigue data and found to be: (Ref. 8)

c = 10-1/3

h = 2-1/3

e = 10/9

The probability of failure is therefore directly proportional to the decisive amplitude to the 10-1/3 power and inversely proportional to the depth to the decisive stress raised to the 1-1/3 power. Thus, the fact that the decisive stress, τ_{rz}, in the hollow ball is greater in magnitude and nearer to the surface (Section 7) will result in a decrease in dynamic fatigue life.

An estimate of the comparative dynamic fatigue life of the hollow ball and the solid ball, for the same probability of survival, may be computed from the relationship:

$$\frac{\tau_H^c \, a_H \, N_H^e}{z_H^{h-1}} = \frac{\tau_S^c \, a_S \, N_S^e}{z_S^{h-1}}$$

$$N_H = \left[N_S^e \left(\frac{\tau_S}{\tau_H}\right)^c \left(\frac{a_S}{a_H}\right) \left(\frac{z_H}{z_S}\right)^{h-1} \right]^{1/e} \quad \text{(millions of stress cycles).}$$

Assuming that the solid ball, subscript S, will endure for one million stress cycles ($N_S = 1.0$):

$$N_H = \left[\left(\frac{123,992}{160,000}\right) \cdot \left(\frac{0.0287}{0.0303}\right) \cdot \left(\frac{0.0096}{0.0101}\right)^{4/3} \right]^{9/10}$$

$N_H = 0.083672$ million stress cycles.

The hollow ball, contact by the Lundberg-Palgren theory, is estimated to have only 8.4% of the life of the solid ball contact when using the maximum reversing orthogonal subsurface shear stress, τ_{rz}, as the "decisive stress amplitude". The stress and depth values were obtained from Table IV.

The maximum, unidirectional subsurface shear stress, τ_{45}, is sometimes mentioned as the "decisive stress" by some rolling element engineers. The relationship based upon τ_{45} and its depth would be:

$$N_H = \left| \left(\frac{186,567}{130,000}\right)^{31/3} \cdot \left(\frac{0.0287}{0.0303}\right) \cdot \left(\frac{0.0160}{0.0134}\right)^{4/3} \right|^{9/10}$$

$N_H = 33.9$ million stress cycles.

The life of the hollow ball would be over 30 times as great as the solid ball if the maximum unidirectional shear stress were considered as the "decisive stress" amplitude.

Normal full-scale bearing data is also reported (Ref. 9) to show that ball bearing life is inversely proportional to the ninth power of Hertz contact stress. (The Lundberg-Palmgren criteria based only upon "decisive stress amplitude" relates life to the inverse 9.3 power of stress. The comparable life of the hollow ball may be estimated as:

$$N_H = \left(\frac{\sigma_{zS}}{\sigma_{zH}}\right)^9 = \left(\frac{579,400}{585,000}\right)^9 = 0.917 \text{ million stress cycles}$$

The life of the hollow ball is 91.7% of the solid ball when based upon maximum Hertz contact stress. These various fatigue life estimates are summarized in Table VI.

Table VI

SUMMARY OF HOLLOW BALL SUBSURFACE INITIATED FATIGUE LIFE ESTIMATES

CRITERION AND DECISIVE STRESS	Hollow Ball Fatigue Life
LUNDBERG-PALMGREN THEORY ORTHOGONAL REVERSING SUBSURFACE SHEAR STRESS (τ_{rz})	8.4% of Solid Ball
UNIDIRECTIONAL STATIC SUBSURFACE SHEAR STRESS (τ_{45})	33.9 times Solid Ball
INVERSE 9TH POWER OF HERTZ STRESS HERTZ CONTACT STRESS (σ_z)	91.7% of Solid Ball

The discussion of "life" has been confined to subsurface initiated fatigue life, however the fatigue life of the spherical shell in reversed bending should also be considered. The stresses on the inner ball surface vary from 150,000 psi tension (Fig. 7) under the load to 4675 psi compression (Fig. 5) at 90° to the applied load. The endurance limit of metals and alloys correlates better with the ultimate strength than with any other properties from static tests. For carbon steels, the ratio of the endurance limit in repeated reversed bending to the ultimate strength varies from 0.45 to 0.55. The physical properties of fully hardened (R_c60) bearing steels (AISI 52100) are not well defined and an SN endurance limit curve is not available. However, we may use reasonable static properties for the hardened steel and assume that the endurance limit in reversed bending is approximately 45% of the yield strength (Table VII).

Table VII

ESTIMATED PHYSICAL PROPERTIES OF BALL BEARING STEEL

AISI 52100 Steel - Rockwell 60C

$Y_{(t)}$	Ultimate tensile Stress (psi)	300,000
S_r	Endurance limit for cycles of completely reversed stress (psi)	135,000

The stress levels and variations of the inner surface of hollow ball are significant with respect to the estimated endurance limits in Table VII. Thus, a finite life which is a function of stress cycles may be anticipated for the hollow ball as a spherical shell. This mode of failure will be competing with the subsurface initiated failure mode to determine the service life of a hollow ball in contact with a flat plate.

SECTION 10

CONCLUSIONS

The results of the current study relate to three distinct areas. First, the method of solution of a contact elasticity problem by the finite element approach is new and the success of the techniques of this type of analysis are worthy of comment. Second, the results of the specific hollow ball analysis and resulting surface and subsurface stress fields will be summarized. Third, the interpretation of the hollow ball stress field deserves comment.

The analysis and resulting three dimensional stress field contained in this report represent a preliminary application of finite element digital computer techniques to the solution of the contact of a specific ball size and wall thickness under a specific normal load. The selection of the specific values and ball size and wall thickness were governed by the availability of one-inch diameter hardened steel balls with a 0.08 inch wall thickness (Ref. 2). Simple compression tests to correlate contact diameter with computed values as a check on the computer solution were possible. The arbitrary selection of 1000 pounds normal load as the maximum load for the analysis will definitely limit the generalization of the analytical results.

10.1 Method of Solution

The successful use of a finite-element general method of representation of a continuous body by a finite number of elements interconnected at a finite number of model points, capable of representing a contact elasticity problem and capable of yielding a description of the complicated three-dimensional stress field has been established.

The use of finite-element types of solutions are of interest because they can solve arbitrary boundary conditions representative of practical engineering conditions which are beyond the present capability of closed-form classical solutions (Sec. 3).

The close agreement of the computer diameter of the circular contact area with experimental results emphasizes the success of this method of general analysis (Sec. 8).

The flat-plate portion of the finite-element solution (Sec. 4) is essentially identical with the classical flat-plate solution of the solid ball case (Sec. 6) and further emphasizes the validity of this type of analysis.

10.2 Hollow Ball Contact Results

The hollow ball shell-bending effects are significant in the determination of the complex three-dimensional stress field in the vicinity of the contact.

The HERTZ contact stresses σ_z, in the contact are only slightly higher for the hollow ball and the maximum value does not occur at the center of the contact (Sec. 7). The hollow ball bending effects result in some relief of the contact stress at the center of contact. (Fig. 22).

The subsurface stress field along the center line of the contact (axis of symmetry, r = 0) is reasonable when compared to a classical solid ball solution. (Fig. 21). The values of the stresses will approach those of the solid ball as the ball wall thickness is increased.

The unidirectional static subsurface shear stress, τ_{45}, is considerably less along the axis of symmetry in the case of the hollow ball (Fig. 21).

The reversing orthogonal subsurface shear stress, τ_{rz}, is greater in magnitude and nearer to the contact surface in the hollow ball solution (Table IV.)

10.3 Interpretation of Results

Estimates of the dynamic fatigue life of the hollow ball contact vary considerably depending upon the criterion or decisive stress amplitude which is selected for the estimate. (Sec. 9 - Table VI). The mode of failure in these estimates is subsurface initiated spalling flakeout type of failure.

Hollow ball bending stresses, especially the variation of stress on the inner wall surface, and repeated cyclic stresses at the hollow ball bond are sources of competing modes of failure for a hollow ball and cannot be safely neglected.

The 33.9 times life increase estimate of contact fatigue life based upon use of the unidirectional static subsurface shear stress, τ_{45}, for the hollow ball is not reasonable and should not be given serious consideration (Sec. 9, Table VI). It is not logical to expect that a weaker hollow ball with significant bending stresses could be capable of such tremendous life increases when compared to a solid ball contact.

A reduction in contact fatigue life for a hollow ball is to be anticipated. The drastic 91.6% reduction estimate when using the Lundberg-Palmgren Theory (Ref. 8) based upon the reversing orthogonal subsurface shear stress as the decisive-stress-amplitude is difficult to accept (Table VI).

The slight 8.3% reduction in contact fatigue life when using Hertz contact stress as the decisive-stress-amplitude is attractive but very optimistic (Table VI).

The stress which should be used as the decisive-stress-amplitude has long been a subject of discussion among bearing engineers. Classical solid-ball type contact fatigue studies have not resolved this question since in classical elastic half-space contact solutions of linear-elastic theory yield maximum values of the various subsurface stresses which are proportional to the Hertz contact stress. The present subsurface stresses vary widely in their relation to the surface Hertz stress and this type of contact of a hollow ball with a flat plate offers a unique opportunity to conduct fatigue life tests and shed additional light upon the most acceptable decisive-stress-amplitude for rolling element bearing fatigue studies.

10.4 Summary

The estimated contact fatigue life of a hollow ball is significantly less (91.6% reduction in life) than solid ball estimates according to currently accepted rolling element fatigue theory (Ref. 8). The specific results quoted are intended to apply only to the specific ball size, wall thickness, and normal load used for the analysis.

Claimed contact fatigue life increases for hollow balls because of their greater elastic contact areas (lower average contact stresses) are suspect.

The results of the specific analysis described in this report should not be interpreted to imply that there are no advantages to be gained from the use of hollow balls in special rolling element bearings. The drastic life-reduction estimates do indicate the significance of the hollow ball bending stresses upon the complex three-dimensional stress field in the vicinity of the contact. Additional analytical study and experimental verification is indicated before optimum use of hollow balls can be anticipated in practical engineering applications. The thin wall of the hollow ball used in this analysis is of academic interest but of little practical interest.

REFERENCES

1. Eklund, Phillip R., Tests on a Three Inch Hollow Ball, Research and Technology Briefs, Vol. IV, No. 10, Oct. 1966 published by U. S. Air Force Systems Command.

2. Final Report on Fabrication Development of Hollow Balls, Technical Report AFML-TR-67-10, February 1967, Air Force Materials Laboratory, Wright-Patterson Air Force Base, Ohio.

3. Harris, T. A., "On the Effectiveness of Hollow Balls in High-Speed Thrust Bearings," ASLE Paper 68 AM 6C-3, A.S.L.E. Transactions, Vol. II Pages 1-5, 1968.

4. "Finite Element Analysis of Axisymmetric Solids (FIRL Version 2) in FEAAS2" - Existing Franklin Institute Research Laboratory Digital Computer Program, Applied Mechanics Laboratory of the Mechanical and Nuclear Engineering Department, Philadelphia, 1967.

5. Belyayev, N. M., Work in the Theory of Elasticity and Plasticity, State Press for Technical Theoretical Literature, Moscow, 1952.

6. Thomas, H. R. and Hoersch, V. A., "Stresses Due to the Pressure of of One Elastic Solid Upon Another", University of Illinois Engineering Experiment Station, Bulletin No. 212, July 1930, Urbana, Illinois.

7. Jones, A. B., Sect. 13 - The Mathematical Theory of Rolling-Element Bearings of Mechanical Design and Systems Handbook, H. Rohbart, Editor, McGraw Hill, 1964.

8. Lundberg, G. and Palmgren, A., Dynamic Capacity of Rolling Bearings, Acta Polytechnica Mechanical Engineering Series Vol. 1 Nr 3, 1947, Royal Swedish Academy of Engineering Sciences, Stockholm, Sweden.

9. Bisson, E. E. and Anderson, W. J., "Advances Bearing Technology" NASA SP-38, Office of Scientific and Technical Information, National Aeronautics and Space Administration, 1964 (pp 383-385).

UNCLASSIFIED
Security Classification

DOCUMENT CONTROL DATA - R & D

(Security classification of title, body of abstract and indexing annotation must be entered when the overall report is classified)

1. ORIGINATING ACTIVITY (Corporate author)
The Franklin Institute Research Laboratories
20th and Parkway
Philadelphia, Pa. 19103

2a. REPORT SECURITY CLASSIFICATION
UNCLASSIFIED

2b. GROUP

3. REPORT TITLE

ANALYSIS OF THE ELASTIC CONTACT OF A HOLLOW BALL WITH A FLAT PLATE

4. DESCRIPTIVE NOTES (Type of report and inclusive dates)
Final Technical Report, 1 January 1968 through 31 May 1968

5. AUTHOR(S) (First name, middle initial, last name)
John H. Rumbarger
R. Clyde Herrick

6. REPORT DATE	7a. TOTAL NO. OF PAGES	7b. NO. OF REFS
January 1969	60	9

8a. CONTRACT OR GRANT NO.	9a. ORIGINATOR'S REPORT NUMBER(S)
F33615-68C-1203	F-C2166-1
b. PROJECT NO. 1315	
c. Task No.	9b. OTHER REPORT NO(S) (Any other numbers that may be assigned this report)
d. 131502	AFFDL-TR-68-123

10. DISTRIBUTION STATEMENT
This document is subject to special export controls and each transmittal to foreign governments or foreign nationals may be made only with prior approval of the Air Force Flight Dynamics Laboratory, FDFM, Wright-Patterson AFB, Ohio.

11. SUPPLEMENTARY NOTES	12. SPONSORING MILITARY ACTIVITY
	Air Force Flight Dynamics Laboratory Wright-Patterson Air Force Base, Ohio

13. ABSTRACT

The objective of this program was to conduct a preliminary analytical investigation of the stress field in a hollow sphere in the vicinity of the contact area. The sphere is subjected to a normal load applied through a flat plate. The elastic contact shape and extent were developed for a load of 1000 lb. applied to a one-inch diameter hollow ball with a 0.08 inch thick wall. Comparison of the maximum value and location of the reversing orthogonal subsurface shear stress with classical solid ball data according to the Lundberg-Palmgren dynamic life theory results in a 91.6% life reduction estimate for the hollow ball contact.

This document is subject to special export controls and each transmittal to foreign governments or foreign nationals may be made only with prior approval of the Air Force Flight Dynamics Laboratory, FDFM, Wright-Patterson Air Force Base, Ohio.

DD FORM 1 NOV 65 1473

UNCLASSIFIED
Security Classification

UNCLASSIFIED
Security Classification

14 KEY WORDS	LINK A		LINK B		LINK C	
	ROLE	WT	ROLE	WT	ROLE	WT
Bearings						
Hollow Balls						
Ball Bearings						
Bearing Life						
Hollow Ball Analysis						

UNCLASSIFIED
Security Classification